Citation
Lacey, A.W. and Chen, W. and Hao, H. 2022. Experimental methods for inter-module joints in modular building structures – A state-of-the-art review. Journal of Building Engineering. 46: ARTN 103792. http://doi.org/10.1016/j.jobe.2021.103792

Experimental methods for inter-module joints in modular building structures – A state-of-the-art review

Andrew William Lacey, Wensu Chen*, and Hong Hao*
Centre for Infrastructural Monitoring and Protection,
School of Civil and Mechanical Engineering, Curtin University, Australia
*Corresponding authors. wensu.chen@curtin.edu.au (W. Chen), hong.hao@curtin.edu.au (H. Hao)

Abstract

This paper presents a state-of-the-art review of the experimental methods for inter-module joints (IMJs) in modular buildings. For the structural response, three levels of study are defined: module (M), frame (F), and joint (J). The joint (J) tests are further classified based on three setups, namely the beam-column (BC) subassemblage with column loading (J/C), the BC subassemblage with beam loading (J/B), and the stub column assembly (J/S). The experimental setups and loading protocols are outlined with reference to the existing literature, and the inherent assumptions and the relative advantages and disadvantages are discussed with the aim of promoting consistency. A case study modular building frame is defined to illustrate the three levels of study (M, F, and J), and the unbraced and braced frames are subjected to lateral loads to demonstrate the effect of bracing on the structural response. The J/C test is shown to be best suited for application to unbraced frames, while the J/S test is more suited to braced frames. Unbraced frames are shown to be vulnerable to failure of the welded beam-to-column connection which can occur in the joint tests before the specimen displacement is large enough to reveal the IMJ behaviour. A summary is given of the existing beam-to-column joint (BCJ) enhancement methods which can strengthen the BCJ and enable measurement of the IMJ behaviour in the tests. The paper concludes with a summary of the experimental methods, recommendations for standardisation, and the key technical challenges and future research directions.

Keywords: Modular building, Inter-module connection, Beam-to-column joint; Loading protocol; Cyclic test

1. Introduction

Modular buildings have great potential as affordable, sustainable, and resilient structures. They have attracted much attention and are promoted as an alternative to traditional on-site construction due to technical advantages including the construction speed, convenience in demounting, reduced environmental disturbance, and better quality of the finished product. As the modules are prefabricated in the factory and assembled on-site to form the complete building, the success of the site installation and the overall structural behaviour are significantly influenced by the connections between the modules. Due to the significance, researchers have proposed new improved inter-module connections (IMCs) and studied their structural responses. However, due to the lack of standards specific to modular buildings, the resulting literature does not consistently apply the same experimental methods. Rather, the experiments vary, and, for example, some studies adopt an IMC specimen, while other studies adopt an inter-module joint (IMJ) specimen incorporating the beam-to-column joint (BCJ).

Following the Eurocode EN 1993-1-8 [1] a joint is defined as the zone in which two or more members are connected.

For structural design, the joint includes each of the components needed to model the structural behaviour given the applied actions. For example, in a traditional steel structure the BCJ includes the column web panel and the adjacent connections. In modular steel structures, the joints between modules are known as the inter-module joints (IMJs). There are three different types of IMJ which can occur in a modular structure depending on the location: corner, end, and internal (Fig. 1). The IMJs are made up of the IMC and the adjacent portions of the columns as shown in Fig. 2 for the (a) vertical and (b) horizontal joints. The BCJ includes the beam-to-column connection and the adjacent portion of the column (Fig. 2a). The length of the IMJ depends on the vertical distance between the floor and ceiling beam centrelines. Vertical space between the beams provides easy access to the IMCs and allows services, e.g., air conditioning ducts, to run between the beams [2, 3]. As will be shown, the size of the IMJ varies among different modular structures. Some structures have a small gap between the beams, while other structures have a very small gap or no gap. Section 3 presents a case study with a dimension of 575 mm between the beam centrelines [4, 5] which is typical of corner-supported modular buildings [6]. Sections 4, 5, and 6 discuss the existing literature in which most of the IMJs have no gap or a very small gap between the beams. Even with zero gap between the beams, however, the distinction between the IMJ and the IMC remains valid, and it can be likened to the BCJ which includes the beam-to-column connection plus a portion of the steel members.

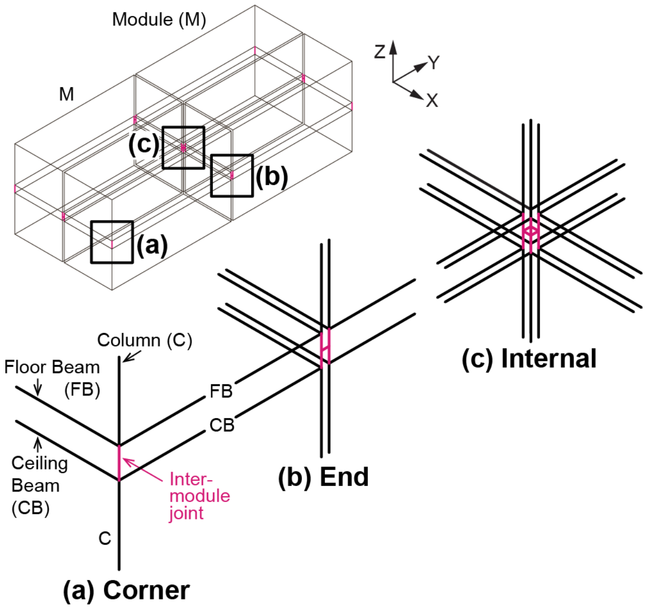

Fig. 1. (a) Corner, (b) end, and (c) internal inter-module joints (IMJs).

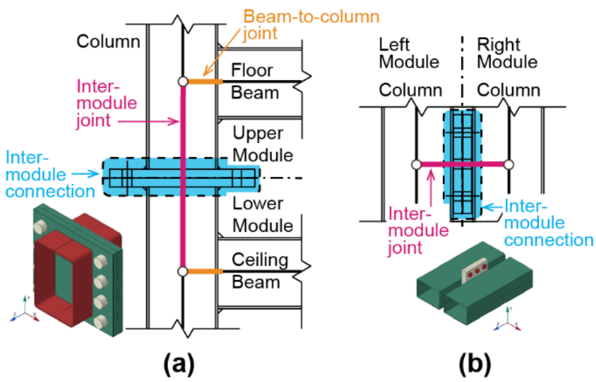

Fig. 2. Inter-module joints (IMJs) incorporating (a) vertical and (b) horizontal inter-module connections (IMCs).

In monolithic construction, e.g., reinforced concrete structures, the joints between elements such as the BCJs might be modelled as either rigid or stiff components. For modular steel buildings, however, the introduction of IMCs introduces the potential for greater deformations which might compromise the structural performance. Shear slip in the IMCs might accumulate over the building height, for example, leading to global failure due to the P-Delta effect. Additionally, compared to traditional steel structures in which the column splice connections might be located away from the BCJ, in modular steel structures the connections between the upper and lower module columns are close to the BCJs (**Fig. 2**a). As a result, the IMC might affect the overall structural response, not only due to its own deformations, but also due to its effect on the surrounding structural elements. Moreover, the deformations of the IMC might be affected by the responses of the surrounding structure. Consequently, when testing the IMC attention should be paid to recreation of the boundary and loading conditions which might affect the resulting structural behaviours. For this reason, some researchers adopt an IMJ specimen incorporating the BCJ, rather than an IMC specimen which requires analysis after testing to assemble the IMJ behaviour.

The development of inter-module joints (IMJs) and connections is outlined in the existing literature by a series of review articles [2, 3, 7-12]. An outline of the relevant background is provided in Section 2 which summarises these review articles (**Table 1**). As will be shown, the selected review articles provide a summary of the existing IMCs and the associated IMJs for modular buildings to date, however, several questions are raised with respect to the selection of the experimental setup to establish the structural behaviour. As will be demonstrated, the structural behaviour of IMJs subjected to lateral loads has been studied at three different levels: module (M), frame (F), and joint (J). At the joint level, the structural behaviour has been evaluated using a beam-column (BC) subassemblage with either column or beam loading (J/C or J/B), and alternatively using a stub column assembly (J/S). Comparing the approach of different researchers (**Table 2**), it is not clear if the different experimental setups produce comparable joint behaviours. Moreover, it is not clear if any one of the setups could be recommended as the best for consistent adoption in future research works. Therefore, the purpose of this review is, firstly, to identify and acknowledge the different practices adopted by different researchers and secondly, to provide guidance as to the inherent assumptions and consequences associated with the use of certain experimental setups.

Table 1. Selected review articles on the development of inter-module joints and connections.

Year	Reference	Title
2018	Lacey et al. [2]	Structural response of modular buildings - an overview
2019	Lacey et al. [3]	Review of bolted inter-module connections in modular steel buildings
2019	Ferdous et al. [7]	New advancements, challenges and opportunities of multi-storey modular buildings – A state-of-the-art review
2020	Srisangeerthanan et al. [8]	Review of performance requirements for inter-module connections in multi-story modular buildings
2020	Deng et al. [9]	Seismic performance of mid-to-high rise modular steel construction - A critical review
2020	Thai et al. [10]	A review on modular construction for high-rise buildings
2021	Nadeem et al. [11]	Connection design in modular steel construction: A review
2021	Chen et al. [12]	Exploration of the multidirectional stability and response of prefabricated volumetric modular steel structures

Table 2. Summary of experimental studies on the performance of inter-module joints. The test types include module (**M**, §4), frame (**F**, §5), and joint (**J**, §6). The joint test sub-types include the beam-column subassemblage with column loading (**J/C**, §6.1) and beam loading (**J/B**, §6.2), and the stub column assembly (**J/S**, §6.5).

Test Type	Year	Reference	Joint Specimen Type	Inter-module Connection Type	Beam-to-column joint enhancement (§6.3)	Axial force included	Illustration
M	2011	Hong et al. [13]	-	-	-	N	Fig. 9(a)
M	2017	Chen et al. [14]	-	Pretension	-	N	Fig. 9(b)
M	2021	Lyu et al. [15]	-	Bolted splice	-	-	Fig. 9(c)
F	2020	Liu et al. [16]	-	Rotary	-	Y	Fig. 10(b)
F	2021	Liu et al. [17]	-	Rotary	-	Y	-
J/C	2017	Chen et al. [18]	Corner	Plug-in	Local plate	Y	Fig. 12(a)
J/C	2017	Chen et al. [19]	Internal	Plug-in	Local plate	Y	Fig. 12(b)
J/C	2018	Sanches et al. [20]	Corner	Post-tensioned	-	Y	Fig. 12(c)
J/C	2019	Cho et al. [21]	Internal	Blind-bolted	Knee brace	N	Fig. 12(d)
J/C	2020	Lee et al. [22]	Corner, Internal	Connector plates	-	N	Fig. 12(e)
J/B	2017	Lee et al. [23]	Corner	Ceiling bracket	-	N	Fig. 14(a)
J/B	2018	Lee et al. [24]	Corner	Ceiling bracket	-	N	-
J/B	2018	Deng et al. [25]	Corner	Welded cover plate	Local plate	Y	Fig. 14(b)
J/B	2018	Deng et al. [26]	Internal	Cruciform bolted	Local plate	Y	Fig. 14(e)
J/B	2019	Dai et al. [27]	Corner	Self-lock	Local plate	Y	Fig. 14(c)
J/B	2019	Wang et al. [28]	Internal	Bolts installed in columns	Local plate	Y	Fig. 14(f)
J/B	2021	Ma et al. [29]	Corner	Side-plate and in-build component	Local plate	N	Fig. 14(d)
J/B	2021	Chen et al. [30]	Corner	Self-locking	Local plate	Y	-
J/S	2018	Liu et al. [31]	-	Bolted flange	-	N	Fig. 18(a)
J/S	2018	Liu et al. [32]	-	Bolted flange	-	Y	Fig. 18(b)
J/S	2019	Chen et al. [33]	-	Rotary	-	N	Fig. 19
J/S	2020	Yang [34]	-	Semi-rigid	-	N	Fig. 20
J/S	2020	Sendanayake et al. [35]	-	Resilient	-	N	Fig. 21
J/S	2021	Lyu et al. [36]	-	Splice connection	-	N	-

After Section 2, this review proceeds as follows. **Section 3** introduces a case study modular building frame which is used to illustrate the three levels of study, i.e., module, frame and joint. A SAP2000 numerical model is defined and the response to a nominal lateral action is discussed to illustrate the different responses of the unbraced and braced frames**. Sections 4**, **5**, and **6** focus on the module, frame, and joint tests, respectively. These sections give a brief overview of the test and a summary of the existing literature, followed by a discussion of the relative advantages, disadvantages, and inherent assumptions. **Section 6** is further divided into subsections on the BC subassemblage with column (J/C) and beam loading (J/B), BCJ enhancement, the effect of module bracing, the stub column assembly (J/S), and specimen scale. **Section 7** reviews the loading protocols adopted for cyclic and monotonic loading in the existing studies. Finally, **Section 8** summarises the existing methods and associated recommendations for future works given throughout this review, and **Section 9** presents the concluding remarks which outline the key technical challenges and future research directions.

2. Development of inter-module joints and connections

Lacey et al. [2] presented a state-of-the-art review of modular structures which was published in March 2018. The existing inter-module connections (IMCs) for modular steel buildings (14 connections) were summarised according to the literature at the time. The current design practice was outlined, including the need for experimental testing which was classified as either proof testing to demonstrate compliance with established performance requirements, or prototype testing to determine the capacity. **Lacey et al. [3]** subsequently presented a further review focusing on the bolted IMCs. The work summarised the existing bolted IMCs (12 connections) and explained the design methods and models in practice at the time (May 2019). The purpose of the IMCs was outlined including to provide a path for load transfer and satisfy robustness requirements, provide local restraint to individual frame members, and to satisfy construction and serviceability requirements. It was noted that vertical space is often provided between the floor and ceiling beams to allow access to the IMCs, and to allow services such as air-conditioning ducts to run between the modules. It was explained how analytical, experimental, and numerical analyses were applied to establish the force-displacement and moment-rotation (M-θ) behaviours of the connections. These structural behaviours could then be simplified and incorporated in global numerical models by applying the presented inter-module joint (IMJ) models. The experimental setups adopted in the existing literature were briefly outlined. The illustrations included experiments on connections to establish the shear force-displacement behaviour and experiments on beam-column subassemblages to establish the M-θ behaviour in combination with an axial load of 10 to 20% of the column yield capacity. The experimental setups were, however, not compared or discussed in detail.

The literature on modular building structures was rapidly expanding and in March 2020, **Srisangeerthanan et al. [8]** presented an updated summary and comparison of the 25 existing IMCs. Key performance assessment criteria were proposed relating to structural, manufacturing, and construction requirements. Specifically, the criteria were: adequacy of the vertical plane axial tensile resistance and horizontal plane (diaphragm) axial and shear resistance, the number of unique parts and their complexity, the complexity of the site-based assembly, the total number of connection components, the ease of shop fabrication, use of self-aligning and self-locking connections, the ease of the site installation, number of operations for site installation, number of tools required for site installation, use of demountable and repairable connections, and the extent of unused space between the modules. The provision of construction and installation tolerances was also mentioned. The 25 connections were rated and ranked based on these 14 criteria, and it was concluded that none were able to fully satisfy the requirements. Therefore, it was recommended that further innovations were required to develop improved connection and framing solutions. Emphasis was placed on the need for automated, i.e., self-locking, connections.

In October 2020, a review by **Deng et al. [9]** was published which focused on the seismic performance of mid-to-high rise modular steel structures. The work outlined the seismic performance, i.e., failure mode, ultimate inter-story drift, and ductility coefficient, of seven existing IMCs, while a further 20 IMCs were mentioned without detailed review of the experiments. The mentioned experiments included subjecting IMJs to axial and bending loads following either a monotonic or cyclic loading protocol. It was reported that the monotonic loading was generally conducted to establish the load transfer mechanism and the M-θ curve, which could be used to classify the connection as rigid, semi-rigid or pinned following Eurocode 3 Part 1-8 [1]. On the other hand, it was indicated that the cyclic loading was undertaken to determine the failure mode, strength, stiffness, ductility, and capacity to dissipate energy. For the seven selected connections, the failure modes included weld fracture, local buckling of a beam or column, and opening of a gap at the IMC. Although the related experiments were outlined, they were not reviewed in detail, and the potential for different structural behaviours depending on the specimen geometry and the loading and boundary conditions was not discussed. The existing simplified numerical models for the seismic behaviour of IMJs were summarised, and it was reported that experiments on the IMCs could lead to the determination of equivalent spring stiffnesses which could be used to model the behaviour of the complete joint. Further, that such spring models could be adopted for the global analysis of modular structures, but that further verification was required to establish the accuracy of the hysteretic behaviour derived in this way. The development of seismic isolation systems was also briefly summarised.

A review by **Thai et al. [10]** was published in December 2020 on the adoption of modular construction for high-rise buildings. The work discussed inter-module joining techniques and their development through the existing literature. The existing steel connections were classified into three groups based on the main component: tie-rod, connector (e.g., self-lock, rotary, and bracket), and bolt. The use of concrete modules was reported to need significant on-site works. This made the site-based construction of concrete modules too slow, hence, concrete modules were not considered further. The new steel connections were briefly summarised, and, although some of the experimental methods were illustrated based on the respective works, they were not compared or reviewed in detail. Numerical models adopted in the existing literature for the IMJs were outlined based on software such as RUAUMOKO and ETABS. This discussion was linked mainly to progressive collapse and structural robustness, and development of the models based on experiments by the respective authors was not discussed. It was reported, however, that the structural behaviour of the IMCs must be incorporated in the global numerical simulation as it can significantly affect the global building behaviour. For design purposes it was reported that steel IMCs are usually classified as semi-rigid with respect to the M-θ behaviour, and that design of the joints is generally based either on Eurocode 3 (Part 1-8) [1] or on AISC 360-16 [37].

The literature on modular building structures continued to expand and in 2021 two relevant review papers were published. **Nadeem et al. [11]** reiterated the basic characteristics of IMCs and identified 16 existing connection details. The behaviours of the IMCs under static and cyclic loadings were outlined with reference to selected existing studies. The key performance indicators were defined and two important parameters were highlighted. First, the displacement ductility factor, i.e., the ratio of the ultimate to the yield displacement, was mentioned as a useful indicator of the capacity to dissipate energy. A ductility factor of 2.5 was reported to indicate good plastic deformability. Second, the initial rotational stiffness was discussed, as it effects the joint classification as rigid, semi-rigid or pinned, and can have a significant effect on the buckling behaviours of the associated members. The present numerical modelling approaches were then summarised, including the existing shear-force slip models for IMCs. Finally, **Chen et al. [12]** gave an updated summary of 41 existing IMC details, which were classified based on the key component: reinforcing rod, connection bloc, bolts, self-centring rubber slider device, and viscoelastic rubbers and SMA bolts. The present design approaches and the existing spring models were outlined.

As indicated in the introduction, the selected review articles [2, 3, 8-12] outline the background and development of IMJs and IMCs to date. It remains, however, to carry out a detailed review of the experimental methods. As will be shown in sections 4, 5, and 6, different researchers have adopted different experimental methods for the IMJs.

Detailed review of the experimental methods is, therefore, required to provide guidance on the different practices and to promote consistency.

3. Case study modular building frame

To illustrate the three levels of experimental study, i.e., module, frame and joint, a typical case study building frame was defined. Considering the typical module dimensions suggested for planning purposes [6] and the module dimensions adopted in the existing case studies [4, 38, 39], a typical 10x4x3 m high module was adopted with a vertical distance between the modules of 0.575 m based on the frame centrelines (Fig. 3). A 150x150x10 mm square hollow section was selected for the beam and column sections, and a post-tensioned (PT) inter-module connection (IMC) [40, 41] was assumed. Two different frames were considered: an unbraced (sway) frame, and a braced frame. The unbraced frame had rigid beam-to-column joints (BCJs), hinged (pinned) column bases and semi-rigid IMCs with defined moment-rotation and force-displacement properties joining the module columns. The braced frame was the same as the unbraced frame, except cross-bracing was added to each module as shown by the dashed line in Fig. 3(a).

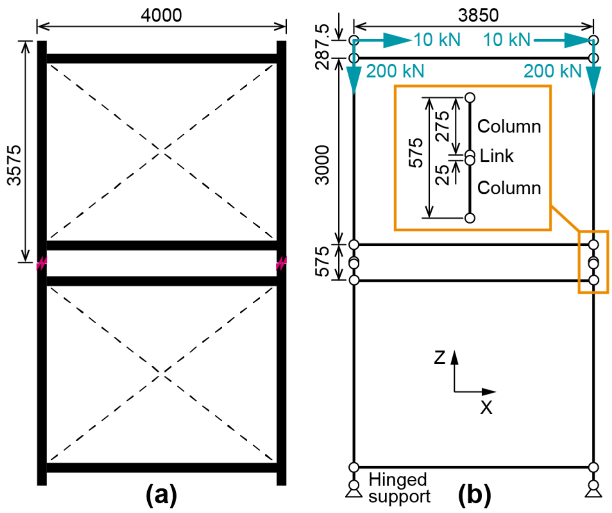

Fig. 3. Numerical model of case study building frame: (a) overall frame dimensions, and (b) centreline dimensions.

Two numerical models were prepared using the software SAP2000. The beams, columns, and braces were incorporated as frame elements, with moments released at the ends of the braces, while each inter-module joint (IMJ) was assembled from two short column lengths and a central nonlinear link element (Fig. 3b). The link elements represented the structural behaviours of the PT connections in the SAP2000 model. The axial force-displacement, shear force-displacement, and bending moment-rotation (M-θ) behaviours of the link (Fig. 4 and Fig. 5) were input following the previous study [5], which estimated the behaviours by applying simplified analytical models [41]. The simplified models were proposed based on the results obtained from the calibrated ABAQUS numerical models. In the present work, an axial force of 0.1Nc was assumed, where Nc is the axial yield capacity of the column, and axial forces of 200 kN were applied at the top of the two upper columns (Fig. 3b). For the purposes of illustration, a nominal lateral load of 10 kN was applied at the top of each column in the upper module (Fig. 3b).

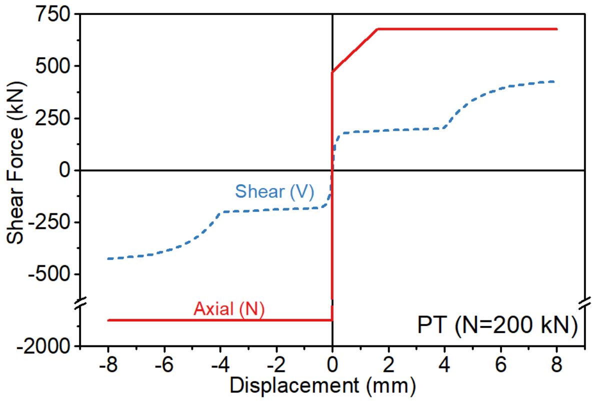

Fig. 4. Axial (N) and shear (V) force-displacement behaviours for the post-tensioned (PT) connection [5].

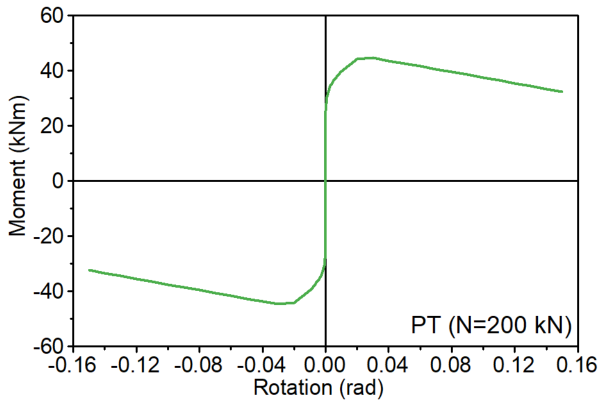

Fig. 5. Moment-rotation (M-θ) behaviour for the post-tensioned (PT) connection [5].

The numerical models were limited to in-plane responses, and nonlinear static analyses were carried out to determine the design actions in the frames. In the unbraced frame the largest bending moment occurred in the beams and columns at the BCJs (Fig. 6a). Unbraced modular frames may, therefore, be vulnerable to failure if the BCJ does not have sufficient strength (Section 6.3) [42]. On the other hand, in the braced frame (Fig. 6b), the beams and columns were subjected to smaller bending moments, e.g., 1.5 kNm compared with 17 kNm. The largest bending moment, e.g., 2.83 kNm, occurred in the IMJs for the braced frame. As can be seen, the IMJs were subjected to similar bending moments in both the unbraced (3.05 kNm) and the braced frames. The bending moment was the smallest in the central nonlinear link which represented the IMC (Fig. 3b), and the largest in the column sections which made up the remainder of the joint. Although the bending moments in the IMJs were relatively small, it should be noted that this was in response to the nominal lateral load applied (Fig. 3b). Larger bending moments can be developed in response to larger lateral forces which may occur, especially at the base of multistorey modular buildings. Consequently, the structural behaviours of the IMJs are of interest as they can significantly influence the overall building response to lateral loads.

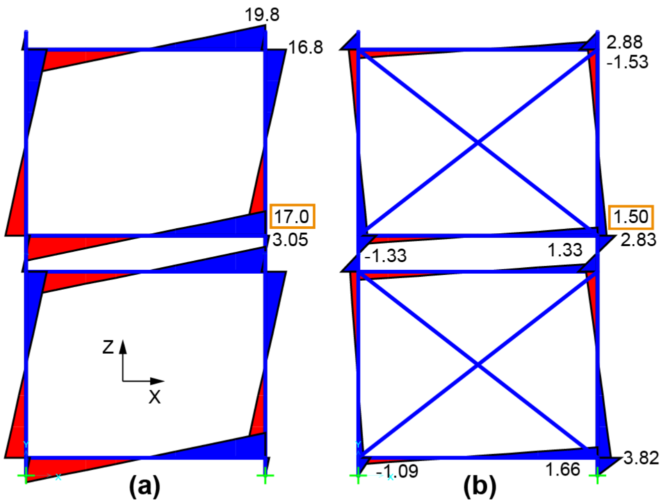

Fig. 6. Bending moment diagrams (kNm) for (a) unbraced and (b) braced case study building fames.

Fig. 7(a) and (b) show the deformed shape of the unbraced and braced frames, respectively. As the lateral displacement for the braced frame was smaller than that for the unbraced frame, Fig. 7(b) has a larger scale factor applied to the displacement than Fig. 7(a). Notwithstanding the different scale factor, due to the prominent vertical displacement in Fig. 7(b) compared with Fig. 7(a), it is evident that the addition of bracing significantly reduced the lateral displacement. Moreover, the displacement of the nonlinear links representing the IMCs (Fig. 3b) was relatively small. Considering the small design actions in the nonlinear links, i.e., less than 10 kN shear force, 3 kNm bending moment, and 200 kN axial force, it can be concluded from Fig. 4 and Fig. 5 that the nonlinear links were responding elastically and did not contribute significantly to the lateral displacement of the frames. The M-θ stiffness of the post-tensioned (PT) connection, for example, was relatively high such that the behaviour of the semi-rigid PT connection did not differ substantially from that of a rigid connection. As will be explained in the following sections, the different responses observed for the unbraced and braced frames can lead to different IMJ behaviours which are best modelled by different subassemblages in the experiments.

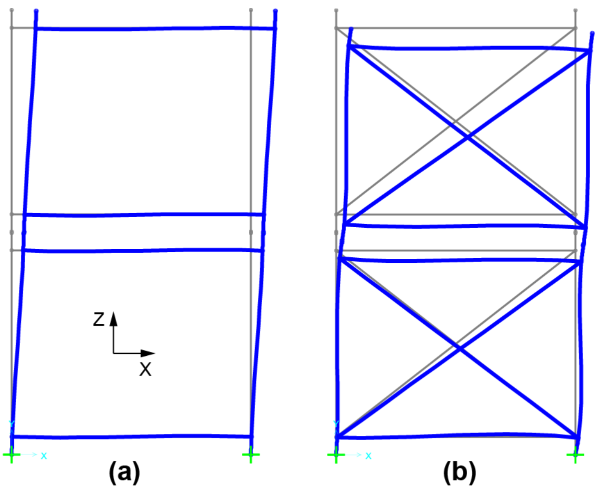

Fig. 7. Deformed shape of (a) unbraced and (b) braced case study building fames.

4. Module (M) test

In the module (M) test (Fig. 8), full scale prototype modules are subjected to axial or lateral loads to simulate the relevant design action in the inter-module joint (IMJ). The tested prototype includes all the main structural elements to reproduce the structural behaviour of an actual modular building as closely as possible. For example, **Hong et al. [13]** tested three full scale stacked modules subjected to lateral loads only, i.e., axial loads were not applied (Fig. 9a). Each module was 6 m long, 3 m wide and 3 m high, and the columns were 125x4.5 square hollow steel (SHS) sections. The reported results included the load-roof drift curve and the corresponding elastic strength and displacement, and ultimate strength and displacement. However, the main interest was the performance of the double skin steel wall panels which provided bracing to the unbraced steel frame and, while the IMJs were included in the specimens, no commentary was given on their performance.

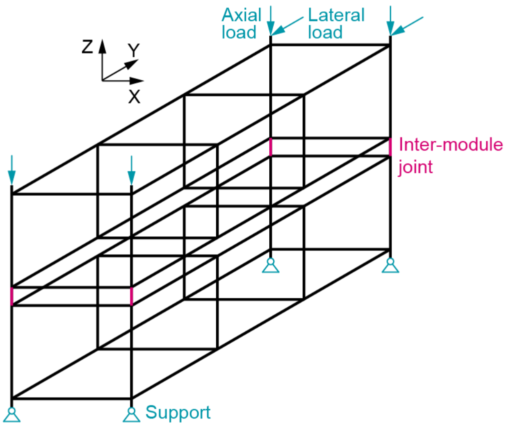

Fig. 8. Module (M) test

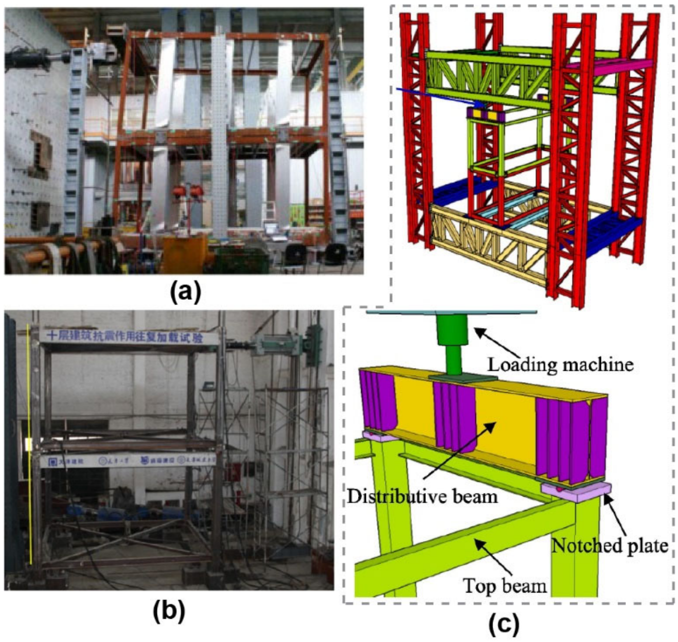

Fig. 9. (a) Lateral loading of stacked modules [13], (b) lateral loading of stacked modules with composite pretensioned connection [14], and (c) reaction frame and axial loading at top of module column [15].

Chen et al. [14] carried out similar experiments in which a lateral load was applied to a two-storey moment-resisting unbraced frame to examine the performance of a pretensioned composite steel-concrete joint between the module columns (Fig. 9b). The modules were 4.5 m long, 3.6 m wide, and 3.0 m high. The columns were 200x8 SHS sections and the floor and ceiling beams were 175x90x8x5 H-beams. The ceiling beams were encased in concrete giving a finished size of 300x200 mm wide, and the columns were filled with concrete and joined by the pretensioned connection. The concrete floor slab was modelled by cross-bracing formed from steel angles installed in-plane at the floor level. Cyclic lateral loading was applied at the top of the second storey module following the Chinese specification JGJ101-96 [43] while the lateral displacement was monitored at the ground, first floor, and second storey ceiling levels. The reported results include the load-upper ceiling displacement curve, inter-storey displacement, gap opening between the module columns, and a description of the failure mechanisms. The damage observed during the experiments included debonding of the concrete ceiling beam from the column face, and cracking and crushing of the concrete ceiling beam adjacent to the column face. Following the initial elastic behaviour, as the applied lateral load was increased, debonding of the concrete surfaces at the inter-module connection (IMC) allowed the upper column to rotate relative to the lower column thereby allowing a gap to open between the columns. However, the largest gap opening was relatively small (0.35 mm), and the measured lateral displacement at the second storey ceiling level was also significantly influenced by damage sustained at the ceiling beam-to-column connection.

In another study, **Lyu et al. [15]** subjected a full-scale two-storey corner supported modular frame to vertical loads to establish the influence of the IMJs on the overall axial behaviour (Fig. 9c). The modules were 6 m long, 2.4 m wide, and 3.0 m high. The columns were 160x8 SHS sections and the floor and ceiling beams were 200x70x6 channel sections. The stacked modules were joined together by bolting the floor and ceiling beams with M16 grade 10.9 bolts, which were tensioned to give an initial preload of 100 kN per bolt. A maximum total axial force of 1307 kN was applied in small increments of 27 kN. Axial load-displacement and load-strain curves were reported for each of the columns, and the failure modes were described. The beam-to-beam splice connections which formed the joints were reported to have little effect on the overall axial behaviour since local deformation and gap opening in the joint initiated after global buckling of the frame.

The preceding examples, which are limited to unbraced frames, show that the prototype specimens and setup are large and, hence, costly in terms of the specimen materials and fabrication, and the equipment and space required for the testing. Consequently, only a small number of specimens are usually tested, e.g., one to three specimens. Although a specimen consisting of two stacked modules may include several IMJs, e.g., one at each corner column, the structural behaviour of each joint may not be completely independent of the other joints. If, for example, one of the joints reaches its yield capacity then the load may be shed to the other joints which, due to the increase in load, may suddenly yield without revealing its own actual yield capacity. This can somewhat diminish the value of the module test as, although several joints may be included in the specimen, they may not be counted to determine the number of units tested for the calculation of statistical parameters, such as confidence intervals.

The prototype module specimens include all the key structural elements and so give an estimate of the joint behaviour including the interaction with other elements such as the beam-to-column joints (BCJs). However, it can be difficult to separate the BCJ and the IMJ behaviours which are combined within the total measured lateral displacement, for example. Still, full-scale testing of complete modules reveals the structural behaviour of the joint incorporated in the whole modular structure. Consequently, compared to the following substructure tests, the module test offers the most accurate assessment of the IMJs and can be recommended on this basis.

5. Frame (F) test

In the frame (F) test (Fig. 10a), prototype frames are subjected to axial and lateral loads to simulate the relevant design actions in the inter-module joints (IMJs). It is assumed that the roof and floor bracing in the complete modules distribute any applied lateral forces to the frames, which can then be studied in isolation. That is, it is assumed that the frames are subjected predominantly to in-plane actions which elicit mainly in-plane responses.

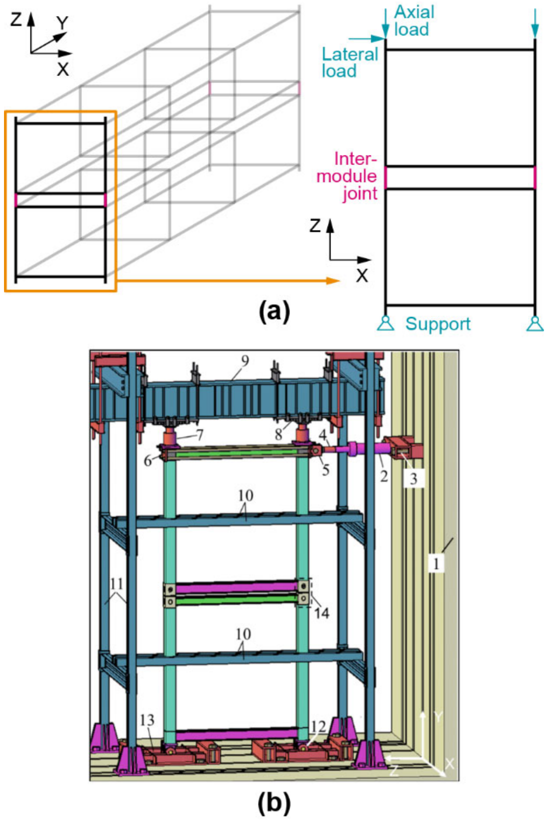

Fig. 10. (a) Frame (F) test, and (b) frame subjected to axial and lateral loads [16].

Two studies were identified which adopted the frame test to study the IMJ behaviour [16, 17]. **Liu et al. [16]**, for example, tested three two-storey frames subjected to axial and lateral loads (Fig. 10b). Each modular frame was approximately 3 m wide and 3 m high. The columns were 200x8 SHS sections, and the floor and ceiling beams were 194x160x6x9 and 150x150x7x10 steel sections, respectively. The stacked frames were joined at the columns by the proposed rotary connection, and the frames were restrained out-of-plane. A constant axial force of 0.2 times the axial force causing first yield of the column sections was applied to the upper frame, after which an in plane lateral force was applied at the top of the upper module. The lateral force was applied using load control with an increment of 10 kN during the initial elastic stage. After the specimen yielded, the test was displacement controlled with 20 mm increments. The in-plane lateral displacement of the frame was measured, and the lateral load-displacement curves were reported for each of the three specimens. Failure modes were also reported and included cracking and local buckling of the floor beam flanges, gap opening between the modular frames at the inter-module connection (IMC), global and local buckling of the corrugated steel panels, tearing of the corrugated steel panel, and fracture of the weld between the corrugated steel panel and the floor beams.

It was reported that the moment-rotation behaviour of the IMCs was affected by the structural configuration and lateral stiffness of the upper and lower modules, i.e., one specimen had no bracing, one specimen had corrugated steel panel bracing to the upper frame only, and one had corrugated steel panel bracing to the upper and lower frames.

When the upper and lower frames had a similar lateral stiffness, the IMCs could be considered as hinged with little moment transfer. On the other hand, if the lateral stiffness of the upper and lower frames were significantly different, the IMC could be semi-rigid with more significant bending moment transferred by the connection. In this way, the joint behaviour can differ between the braced and unbraced structures, which should be considered when planning tests to ascertain the IMC or IMJ behaviour.

From the preceding study [16], it can be seen that, similar to the module (M) test, the frame (F) test specimens and setup are also large and, hence, costly in terms of the specimen materials and fabrication, and the equipment and space required for the testing. However, the frame (F) specimens are smaller and so more cost effective than the module (M) specimens. Moreover, the frame specimens include the key structural elements related to the in-plane response of the frame and so give a reasonable estimate of the joint behaviour in this context. Again, it can be difficult to separate the component behaviours which combine to give the total lateral displacement. Nevertheless, the frame (F) test can be recommended as it captures the structural behaviour of the joint incorporated within the frame. In the complete modules, out-of-plane stability is provided to the frame by the other structural elements, i.e., the bracing and perpendicular frames. When the frames are considered in isolation additional supports are required to ensure out-of-plane stability, and to limit the structural response to the in-plane behaviour. In this way, study of the frame substructure neglects global failure modes which might occur in the complete three-dimensional structure, and the existing study [16] is limited to the response of a modular frame in the XZ plane (Fig. 10(a)).

6. Joint (J) test

6.1. Beam-column subassemblage with column loading (J/C)

In the joint (J) test (Fig. 11), a beam-column subassemblage is adopted which incorporates the inter-module joint (IMJ) in addition to a portion of the adjacent columns and beams. The lengths of the column and beam segments are determined based on the points of inflection, i.e., the points at which the bending moment is zero, in an unbraced modular frame subjected to a lateral load (Fig. 11). Thus, half of the full column and beam lengths are included in the subassemblage so that the design actions in the specimen are equivalent to those in the full frame. For example, Fig. 11(a) shows the bending moment diagram for the full frame in the transverse XZ plane and Fig. 11(b) shows the bending moment diagram for the subassemblage. For the column loading, i.e., J/C, the lower column and beams are restrained while axial and lateral loads are applied to the top of the upper column.

The J/C test has been adopted by several researchers to study the in-plane response of corner and end joint specimens with small or zero gap between the floor and ceiling beams [18-22] (Fig. 12). For example, **Chen et al. [18]** applied quasi-static uniaxial monotonic and cyclic loads to a corner joint specimen which incorporated a plug-in device and beam-to-beam bolts (Fig. 12a). The 2/3 scale prototype joint specimens were nominally 2 m tall and 2 m wide, and consisted of 150x8 SHS columns, 150x8 or 150x250x8 beams, and 10 mm thick stiffeners to the welded beam-to-column joints (BCJs) of selected specimens. The base of the lower column was restrained against translation while in-plane rotation was permitted. The beams were restrained against vertical translation while horizontal translation and rotation were permitted by rollers. At the top of the upper column the axial load was applied by a hydraulic jack. Rollers were provided such that lateral translation of the jack was permitted while the axial force was maintained.

The lateral (horizontal) force was applied using a hydraulic jack which was connected to the upper column with a pinned connection which allowed rotation. Two specimens were subjected to a quasi-static monotonic lateral load which were combined with a constant axial force of 0.2 times the yield capacity of the column. Four specimens were subjected to a quasi-static cyclic lateral force according to JGJ101-96 [43] in addition to the constant axial force of 0.1 or 0.2 times the column yield capacity. In each test the lateral displacement was measured at the upper column end where the load was applied, and at the end of each beam. For the monotonic loading, the load-displacement curves were presented, and the failure modes were described with each specimen experiencing failure of welds at the BCJ. For the cyclic loading, the hysteretic performance and skeleton (load-displacement) curves were presented. The failure modes were described and included fracture of welds at the BCJ, local buckling of the column at the BCJ, and the opening of a gap at the inter-module connection (IMC). The results demonstrated that the deformation capacity of the IMJ was significantly influenced by the stiffness of the BCJ.

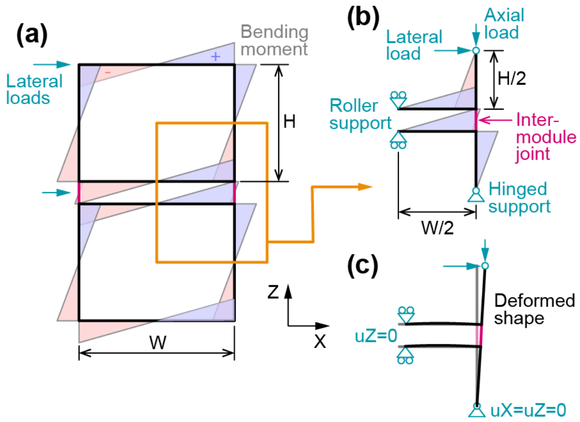

Fig. 11. (a) Unbraced frame showing bending moment, (b) beam-column subassemblage with column loading (J/C) showing bending moment, and (c) deformed shape of the beam-column subassemblage.

Chen et al. [19] extended the work by applying similar monotonic and quasi-static cyclic lateral loads to an internal IMJ (Fig. 12b). Again, the lateral deformation of the IMJ was closely influenced by the stiffness of the BCJ. It was reported that a gap could open between the upper and lower columns, and the observed failure mechanisms included cracking of the beam-to-column weld and tensile failure of the BCJ stiffeners which were introduced to improve the BCJ performance (Section 6.3).

Sanches et al. [20] applied a constant axial load equal to 0.17 times the column yield capacity and a cyclic lateral load according to AISC 341 [44] to corner joint specimens (Fig. 12c). The joint specimens were nominally 3.345 m tall and 1.75 m wide, and consisted of a W 150x18 floor beam, a W100x19 ceiling beam, and two 127x6.4 SHS columns which were joined by a pre-tensioned 25.4 mm diameter rod. The setup adopted was different to those mentioned previously in two ways. First, the joint specimen was rotated from vertical to horizontal, and it was tested at the ground level. Second, the axial load was applied by a jack at the base of the bottom column, while the lateral load was applied by an actuator at the top of the upper column. A spherical support was placed on a roller to create a guided spherical bearing support at the top of the upper column, i.e., lateral displacement was permitted but it was limited to in-plane free sliding, while the spherical support permitted free rotation. At the bottom of the lower column, only a spherical support was provided to permit rotation while restraining translation. A roller boundary support was provided at the end of the beams. Strain gauges were installed across regions of high strain on the specimens and linear variable differential transformers were adopted to measure the in- and out-of-plane displacement of the columns and beams. The hysteretic performance and skeleton (load-displacement) curves were presented. Notwithstanding the apparently different experimental setup, similar failure modes were reported including cracking of the floor beam-to-column welds for which enhancement of the beam-to-column connection was recommended (Section 6.3).

In another example, **Cho et al. [21]** adopted a different setup which used hinged supports instead of roller supports for the beams in an internal specimen with a blind-bolted connection (Fig. 12d). Hinged struts were added to support each of the two lower beams. The upper and lower beams on each side were then joined by a vertical link plate which was loosely connected by a single bolt at each end to allow rotation. In this way, translation of the lower beam was permitted, however, it was constrained to follow an arc with a radius equal to the length of the hinged strut. Similarly, relative translation between the upper and lower beams was permitted, however, translation of the upper beam relative to the lower beam was constrained to an arc with a radius equal to the length of the hinged vertical link plate. It was reported that these restraints allowed a rigid body rotation of the entire specimen which caused an additional lateral displacement at the top of the upper column. That is, lateral displacement of the beams was accompanied by a corresponding vertical displacement due to the constraint. Therefore, the vertical displacement was measured at the beam ends, and the rigid body rotation and corresponding lateral displacement at the top of the upper column was calculated and subtracted from the total measured lateral displacement. In this way, it was reported that the hinged beam restraints could be adopted without significantly affecting the behaviour of the subassemblage.

Use of hinged struts to support the beams simplifies the experimental setup by eliminating the roller supports and the corresponding reaction frames which would otherwise be required to restrain each of the beam ends against vertical translation. However, despite their use in the referenced study [21], hinged beam supports are not recommended for three reasons. First, while the lateral displacement of the column might reach 100 mm or more in a typical specimen, the vertical displacement of the beam end could be only 0.5 mm. Such a small displacement could be difficult to measure accurately and could lead to an inaccurate estimate of the lateral displacement of the column. Secondly, if an axial force is applied to the column during the test, the lateral deformation of the column due to the hinged beam support will have an associated P-Delta effect. Hence, the lateral deformation of the column cannot be estimated based only on the vertical displacement of the beam. Thirdly, the use of hinged rather than roller beam supports can influence the design actions transferred to the IMJs and, hence, the structural behaviour recorded for the IMJs.

Among the existing studies, two different cases of restraint for the top of the column were considered. The studies which included an axial force applied to the upper column [18-20] generally provided a hinged roller restraint at the top of the column. In one study a spherical bearing was combined with a roller support, and in two studies only a roller support was provided and the hydraulic jack to column connection was considered to permit sufficient rotation to justify its classification as a hinged connection. Out-of-plane horizontal translation of the upper column was constrained by the rollers which allowed only in-plane horizontal translation. The studies which did not include an axial force [21, 22] generally left the top of the column free (Fig. 12d and e). As the axial deformation of the specimen can affect the structural behaviour of the joint [5, 41, 45], it is recommended that an axial force of 0.1 to 0.3 times the yield strength of the column section [3, 19] should be included in the joint test to obtain the most realistic joint behaviour. This is because the largest shear forces occur in the IMCs at the base of the building where the axial forces due to self-weight are the largest [5]. Hence, although smaller axial compression forces and axial tension forces are possible, they are typically associated with smaller shear forces. Therefore, the first case is recommended wherein some restraint is provided to the top of the upper column by way of application of the axial load.

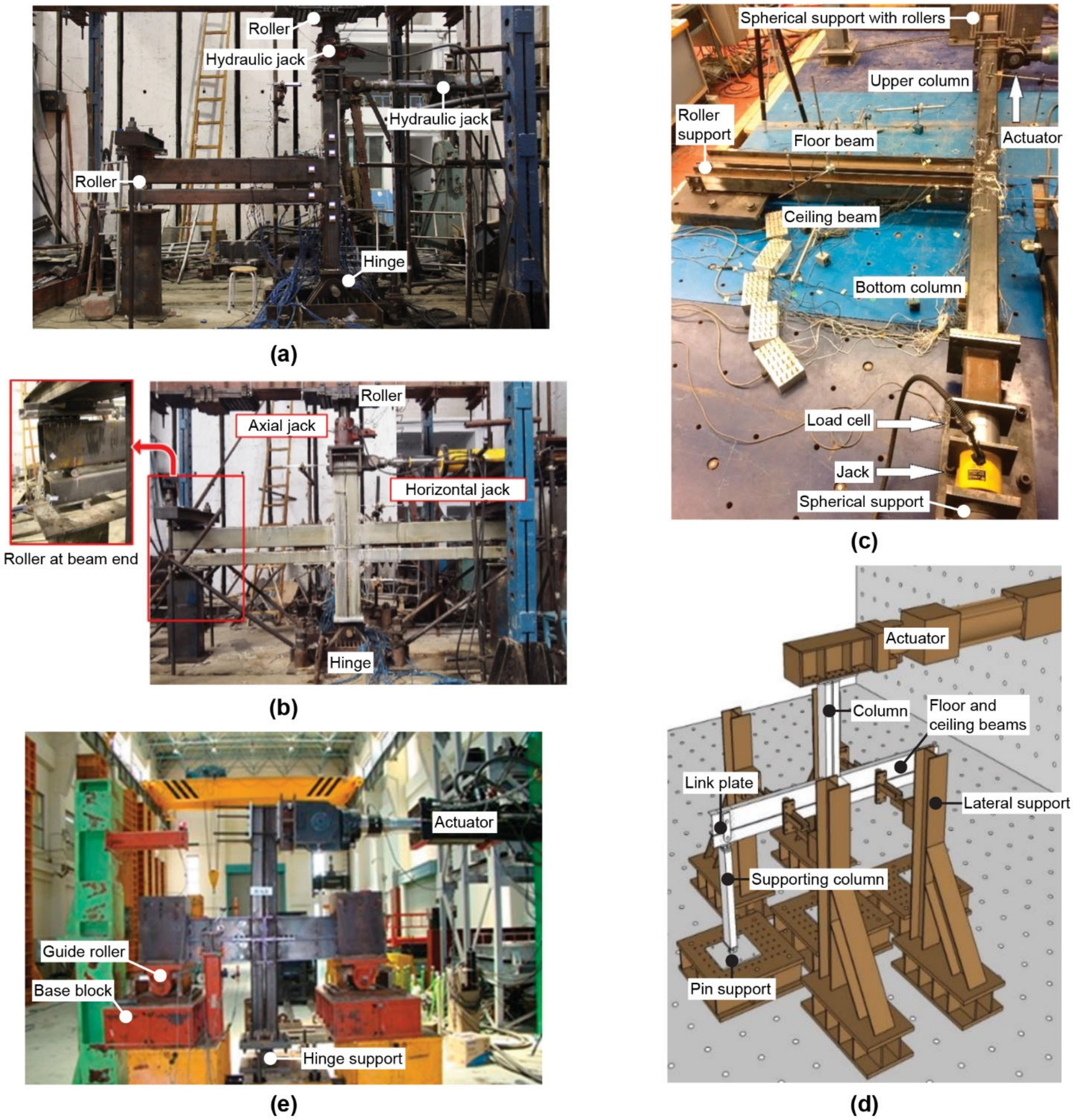

Fig. 12. Beam-column subassemblage with column loading for (a) corner specimen [18], (b) internal specimen [19], (c) corner specimen with post-tensioned modules [20], (d) internal specimen with blind-bolted connection [21] and (e) internal specimen with connector plates [22]. Annotation revised and added for clarity.

The beam-column subassemblages are substantially smaller than the preceding module and frame specimens, hence, the joint tests can be seen to be more cost effective in terms of the specimen materials and the equipment required for the tests. Moreover, the joint tests allow an assessment of the IMJ behaviour including the effect of the BCJs. However, the geometry of the joint specimen is determined by the geometry of the modular frame (Fig. 11) and, since it is derived based on the points of inflection in the unbraced frame in the transverse XZ plane, the corresponding behaviours are specific to the unbraced transverse frame geometry. The unbraced modular frame must, therefore, be defined before the joint test can be carried out, and it should be noted that the joint test reveals the structural behaviour of the IMJ in the context of the defined substructure. In addition, the displacement and ultimate failure of the joint specimen may be determined primarily by the BCJ and by the size of the beam and column sections, rather than the IMJ itself. Enhancement of the BCJ may, therefore, be beneficial to reveal the behaviour of the IMJ. On the other hand, if the aim of the experiments is to ascertain the failure modes of prototype IMJs including the BCJs, then enhancement of the BCJ may be necessary to enable adequate performance (Section 6.3).

6.2. Beam-column subassemblage with beam loading (J/B)

The joint test with beam loading (J/B) is the same as that with column loading (J/C), however, the lateral load is applied to the free end of the beams while the axial load is applied to the top of the upper column which is laterally restrained. Fig. 13(a) shows the bending moment diagram for the beam-column subassemblage with beam loading, and Fig. 13(b) shows the corresponding deformed shape of the specimen.

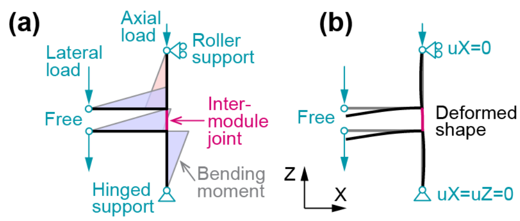

Fig. 13. (a) Beam-column subassemblage with beam loading (J/B) showing bending moment, and (b) deformed shape of the beam-column subassemblage.

The J/B test has been adopted by several researchers to study the in-plane response of corner and end joint specimens with small or zero gap between the floor and ceiling beams (Fig. 14) [23-29]. For example, **Dai et al. [27]** adopted a joint test with beam loading to establish the moment-rotation (M-θ) behaviour of the plug-in self-lock joint for modular buildings (Fig. 14c). The full-scale prototype joint specimens were nominally 3.61 m tall and 1.97 m wide, and consisted of 200x10 SHS columns, 200x180x8 rectangular hollow section (RHS) or 200x180x6x10 H floor beams, 200x180x6 RHS or 200x180x6x8 H ceiling beams, and 8 mm thick plate stiffeners to the beam-to-column joint (BCJ). A small axial force of 0.05 times the yield capacity of the column was applied at the top of the upper column using a hydraulic jack. The lateral (vertical) force was applied using a hydraulic jack which was connected to the free end of the beams with a pinned connection to allow rotation. Eight joint specimens were tested. One specimen was subjected to the axial force in addition to a quasi-static monotonic load applied to the beams. Seven specimens were subjected to the axial force plus a quasi-static cyclic load which was displacement controlled according to ATC-24 [46] and AISC 341 [37]. Lateral displacement of the beams and columns was measured by linear variable differential transformers while strain gauges were installed to monitor high strain areas on the specimens. For the specimen subjected to monotonic lateral loading the moment-drift ratio curve was presented along with a description of the failure modes including local buckling of the beams, development of a plastic hinge in the upper beam, and opening of a 3 mm vertical gap on one side of the inter-module connection (IMC). For the specimens subjected to cyclic lateral loading the hysteretic moment-drift ratio curves were presented and the cyclic envelope curves were determined. The failure modes were also discussed including local buckling and cracking of the beams, weld failure and opening of a gap at the IMC for the specimens with hollow section beams. In contrast, the specimens with H section beams exhibited local buckling of the flanges of the beams without any fracture or cracking. M-θ curves were derived for the inter-module joint (IMJ) by subtracting the rotation of the beam relative to the ground from the rotation of the column relative to the ground. Hence, an M-θ curve was presented for the specimen with monotonic loading, and similar cyclic envelope curves were presented for the specimens subjected to cyclic loading.

In another example, **Ma et al. [29]** subjected three end joint specimens to monotonic beam loading (Fig. 14d). The full-scale joint specimens were nominally 1.75 m tall and 1.5 m wide, and consisted of 150x8 SHS columns, 250x140x10 or 200x140x10 cee section beams, and 12 mm thick plate stiffeners to the BCJ of one specimen. The lateral (vertical) force was applied to the beams using a centre hole hydraulic cylinder. No axial force was applied to the specimen. Displacement gauges were adopted to measure the lateral displacement of the beams and columns, and strain gauges were installed to measure strain on the surface of the specimen. Digital image correlation (DIC) was also successfully adopted to measure displacement of the visible front side of the IMJ throughout the loading sequences. Despite the successful use of DIC to measure displacements in experiments on IMCs [40, 47, 48], this was the only study which took advantage of the technology for the IMJs. M-θ curves were reported for each of the three specimens based on the lateral (vertical) displacement of the beams at the loaded end. The failure modes were also reported and included cracking of the weld at the BCJs and local buckling of the beam flange.

The J/B test is the most adopted joint test with eight existing studies applying the test, as compared with five studies applying the J/C test (**Table 2**). It is understood that beam loading is more popular than column loading due to the simpler experimental setup. In the J/B test the axial force is applied to the column while the lateral (vertical) force is applied to the beams. Consequently, there is no need for a complex roller support at the top of the column. Despite its popular use, the J/B is not recommended by this review. The J/B test is like the J/C test because the loading and boundary conditions can produce the same distribution of design actions such as the bending moment throughout the specimen. This can be seen by comparing Fig. 11(a) and (b) with Fig. 13(a). However, due to the different boundary conditions, i.e., top of column restrained for the J/B test, the deformed shape of the specimens is different, as can be seen by comparing Fig. 11(c) and Fig. 13(b). As a result, the J/B test cannot reproduce nonlinear effects such as the P-Delta effect. Moreover, the structural behaviour of the IMJ could be affected by the deformed shape of the specimen [41, 45]. Therefore, even if the experimental results are only used to calibrate a corresponding numerical model, the J/B test may not be sufficient because the different deformed shape can change the active components which can lead to different load transfer mechanisms. It should be noted that such observations, i.e., the J/B test produces a different deformed shape and cannot reproduce nonlinear effects, are not specific to modular structures and have been reported previously for reinforced concrete beam-column joints [49], for example. In the context of modular buildings, it is recommended that the beam loading setup should only be applied to determine the structural behaviour of IMJs if it can be demonstrated that the structural behaviour of the IMJ is not affected by the deformed shape of the specimen.

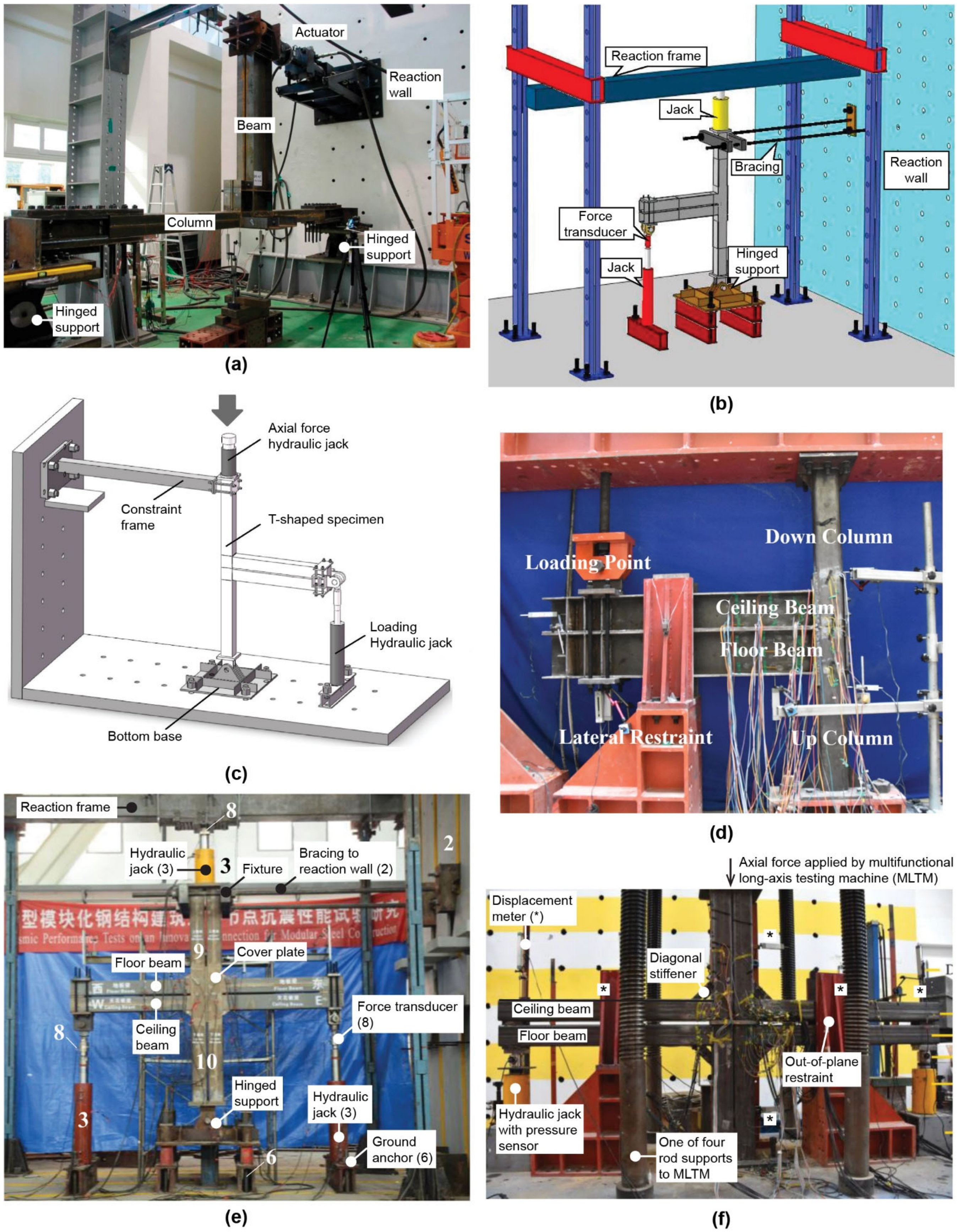

Fig. 14. Beam-column subassemblage with beam loading for specimen with (a) ceiling bracket [23], (b) welded cover plate [25], (c) self-lock connection [27], (d) novel connection with superimposed beams [29], (e) cruciform bolted connection where 9 is the upper module and 10 is the lower module [26], and (f) connection with bolts installed in the columns [28]. Annotation revised and added for clarity.

6.3. Beam-to-column joint (BCJ) enhancement

In modular buildings the beam-to-column joints (BCJs) are prone to early failure, irrespective of the experimental setup, i.e., module, frame, or joint test. For a composite steel-concrete frame **Chen et al. [14]** reported debonding of the beam from the column face and cracking and crushing of the beam adjacent to the column face (Section 4). On the other hand, for modular steel buildings, the beams are often connected to the columns by welding. The resulting welded BCJ is vulnerable to cracking [18, 19] (Section 6.1). Fracture of the welded joint is a critical failure mechanism which reduces the specimen stiffness and ultimately leads to complete failure [42]. As mentioned in Section 3, the unbraced modular frame is subjected to the largest bending moment at the BCJ. Apart from stress concentration at the welded connections, this explains why the unbraced modular structures are particularly vulnerable to failure at the BCJ.

Two main approaches are noted in the existing literature to address the potential for failure at the BCJ: local plate strengthening, and knee bracing. The first approach is to install plates to locally strengthen the beams at the BCJ. Due to the requirement to carry axial loads, the columns are generally constructed from larger or thicker steel sections than the steel beams. Therefore, failure of the BCJ begins, for example, by cracking of the beam-to-column weld at the corner of the beam, i.e., the failure begins in the beam rather than the column. The crack propagates vertically through the beam section along the beam-to-column weld which leads to premature failure. The local plate strengthening approach is successful as it shifts the plastic hinge developed in the beam from the vulnerable beam-to-column weld to the edge of the strengthened beam section.

For example, **Deng et al. [25]** proposed two 100x70x10 mm thick triangular plate stiffeners (Fig. 15a). The smaller 70 mm length of the stiffeners was welded to the face of the 200x10 SHS column. The longer 100 mm length was welded to the face of either the 200x6 SHS ceiling beam or the 200x8 SHS floor beam depending on the position of the stiffener. For the monotonic lateral loading (J/B with axial force), the specimens without stiffeners encountered local buckling of the beams at the interface with the column and fracture of the weld between the beam and the column. On the other hand, the specimen with the stiffeners included encountered local buckling of the beams at the edge of the plate stiffeners and fracture of the weld between the stiffeners and the column. For the cyclic lateral loading, the specimens without stiffeners failed due to fracture of the beam-to-column welds which initiated at the beam corners and propagated vertically through the beam webs and column face. The failure was brittle and use of the connection without stiffeners was not recommended except for applications with low seismic loads. In contrast, the specimen with stiffeners exhibited a higher initial rotational stiffness and a ductile failure. The ductile failure occurred as the plastic hinge which developed in the beams was moved 100 mm away from the column face to the edge of the 100x70x10 mm stiffener. Due to the small inelastic deformation capacity the unstiffened connections were only suitable for ordinary moment frames (OMF) according to AISC 341 [37], whereas joints with the stiffeners could be adopted in special moment frames (SMF) due to the increased capacity for inelastic deformation.

Dai et al. [27] proposed two different methods: 100x100x8 mm thick triangular plate stiffeners known as rib stiffeners (Fig. 15b) and 200x200x10 mm thick cover plates (Fig. 15c). The specimens were constructed from 200x10 SHS columns, 200x180x8 RHS or 200x180x6x10 H floor beams, and 200x180x6 RHS or 200x180x6x8 H ceiling beams (Section 6.2). The plate stiffeners were welded at the BCJ, and they were aligned with the web(s) of the beams. Hence, two stiffeners were provided at each BCJ for specimens with RHS beams, and one stiffener was provided for specimens with H beams. For the cover plate detail, a cover plate was welded to the upper and lower flanges of the beam adjacent to the BCJ. Local buckling and cracking of the beams was shifted away from the column face to the edge of the rib stiffeners (Fig. 15b), or 90 to 120 mm from the edge of the cover plates (Fig. 15c) due to the greater constraint effect. The maximum strength of the joints with cover plates was up to 12% greater than the strength of the joints with rib stiffeners. Hence, the cover plates were recommended over the rib stiffeners, especially as the cover plates took up less space at the corner and effectively reinforced the upper and lower beam flanges.

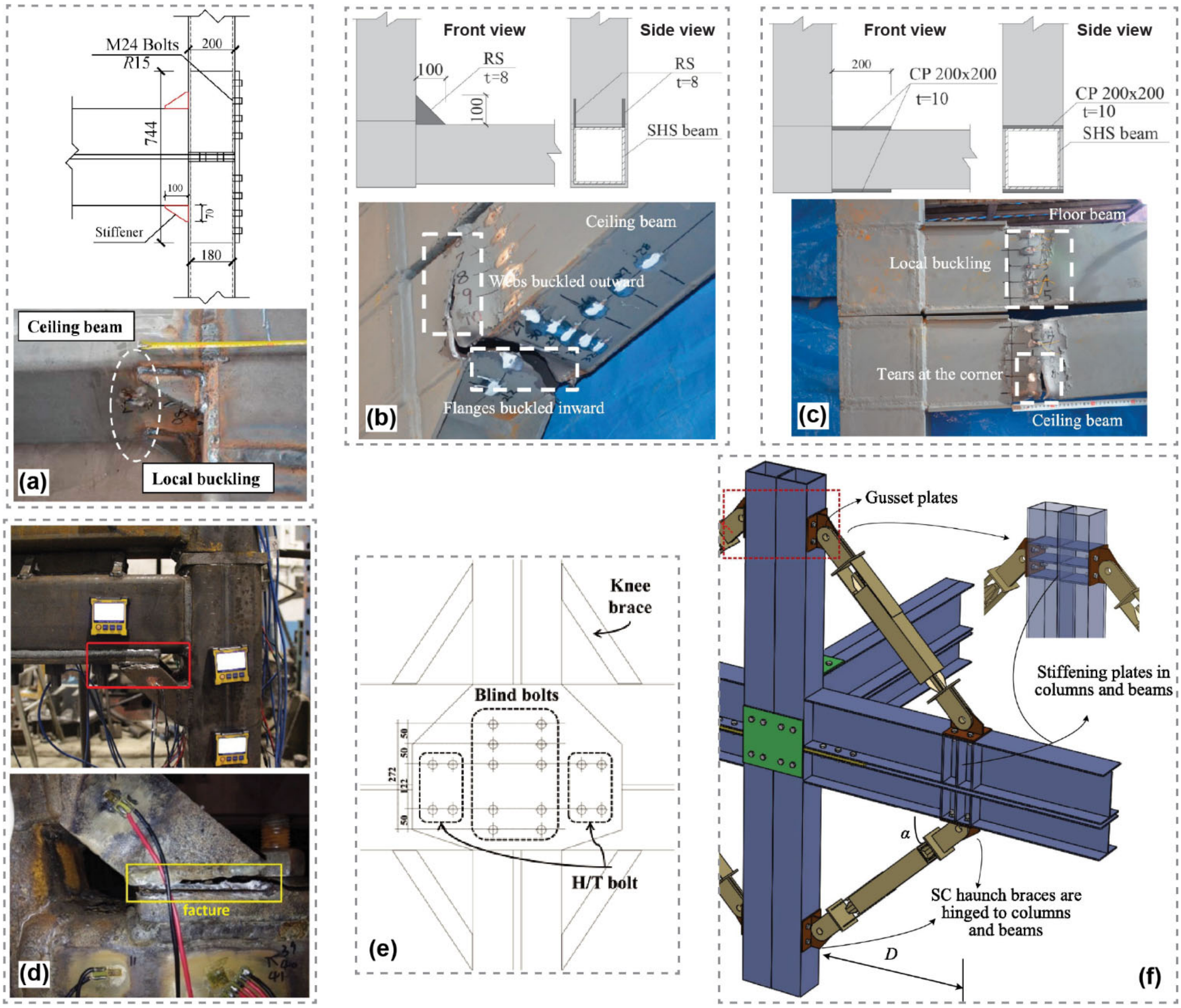

Fig. 15. Beam-to-column joint (BCJ) enhancements: (a) 2-100x70x10 mm plate stiffeners and example failure mechanism [25], (b) 2-100x100x8 mm rib stiffeners (RS) and example of failure mechanism [27], (c) 2-200x200x10 mm cover plates (CP) and example failure mechanism [27], (d) 2-10 mm thick diagonal plate stiffeners with weld fracture highlighted [18], (e) L50x50x4 knee brace [21] and (f) Self-centering (SC) haunch brace [50].

Chen et al. [18] and **Chen et al. [19]** proposed two 10 mm thick diagonal plate stiffeners (Fig. 15d). At one end the plate stiffeners were welded to an 80x150x16 mm thick plate which was in turn welded to the face of the 150x8 SHS column. At the other end, the plate stiffeners were welded to a 430x150x16 mm thick plate which was in turn welded either to the floor beam or to the ceiling beam depending on the stiffener location. The diagonal stiffeners increased the stiffness and strength of the joint specimen; however, fracture of the stiffener welds was a prominent failure mechanism which could reduce the ductility compared to specimens without the stiffeners.

The second approach is to install knee bracing at the BCJ. The knee bracing is larger than the local plate strengthening, and its success is in part due to its ability to reduce the bending moment at the BCJ. For example, the knee brace can transfer axial forces from the beam to the column, leaving the BCJ subjected only to axial and shear forces. For example, **Cho et al. [21]** proposed knee braces constructed from 50x4 equal angle sections (Fig. 15e). The braces were welded to the 200x100x6 RHS column at one end, and the C250x100x4 floor beam or the C150x100x4 ceiling beam at the other end. With the knee braces installed the first yielding occurred in the floor and ceiling beams, followed by local buckling of the ceiling beam, and finally the specimen failed by buckling of the knee braces and floor beams. However, the knee braces increased the initial force-displacement stiffness by a factor of 2 and the peak lateral force by a factor of 1.6, and, hence, were reported to be very effective. As another example, **Zhang et al. [50]** proposed a self-centering (SC) haunch brace (Fig. 15f). The SC haunch brace increased the lateral stiffness throughout the loading and improved the bearing and SC performance. It remains, however, to carry out experiments to verify the numerical performance of the proposed bracing.

Overall, both local strengthening and knee bracing can address the potential for failure at the BCJ. As the BCJs are prone to early failure, the BCJs in a joint specimen may fail before the lateral load is increased to a value large enough to reveal the IMJ behaviour. Therefore, it is recommended that the BCJs should be strengthened by either approach to allow the joint tests to reveal the IMJ behaviour. From another perspective, strengthening of the BCJ is required in the actual modular structure to address the potential for failure. Therefore, the strengthened BCJ must be incorporated in the joint specimen to reflect the actual modular structure. Although the strengthening of the BCJ can change the IMJ behaviour measured in the joint test, the measured IMJ behaviour is expected to reflect that of the actual structure.

6.4. Effect of module bracing

Modular building frames can be braced or unbraced. Although the majority of the existing studies on the inter-module joint (IMJ) focus on the behaviour of unbraced frames, braced frames are commonly adopted in practice and in the existing case studies [51]. It is, therefore, appropriate to consider if the typical beam-column (BC) subassemblage test can be applied in the case of braced frames. Module bracing changes the load path through the modular frame (Section 3). Consequently, a braced frame has a different bending moment diagram than an unbraced frame (Fig. 6). Comparing Fig. 11 and Fig. 13 with Fig. 16 it can be seen that the BC subassemblage with either column or beam loading is not able to reproduce the bending moment diagram of the braced frame. Therefore, the BC subassemblage cannot be adopted to accurately capture the joint behaviour within a braced modular frame.

Different joint behaviours are expected for the braced and unbraced frames, which can be explained with reference to the case study frame introduced in Section 3. Comparing the bending moment diagrams for the unbraced and braced frames, it can be seen that the presence of bracing affects the design actions to which the IMJ is subjected. In the unbraced frame (Fig. 6a) the beam-to-column joint (BCJ) is subjected to a large bending moment such that the measured lateral displacement of the specimen is significantly influenced by the BCJ. In contrast, in the braced frame (Fig. 6b), the BCJ is subjected to a smaller bending moment, which affects the lateral displacement of the specimen due to the smaller BCJ response. As the BCJ has less effect on the lateral response of braced frames, there is growing interest in experimental setups which do not include the BCJ, which is discussed further in Section 6.5. Comparing the deformed shape of the unbraced and braced frames, the unbraced frame (Fig. 7a) is subjected to larger lateral displacement, while the braced frame (Fig. 7b) exhibits smaller lateral displacement and a more prominent axial deformation. The different deformed shape of the frames leads to different deformed shapes for the IMJs, which can affect the structural behaviour. In addition, while the above discussion refers to elastic analyses, it should be noted that the introduction of bracing to a modular frame can affect the nonlinear frame response, e.g., change the sequence of component failure, thereby affecting the design actions applied to, and the response of the IMJs.

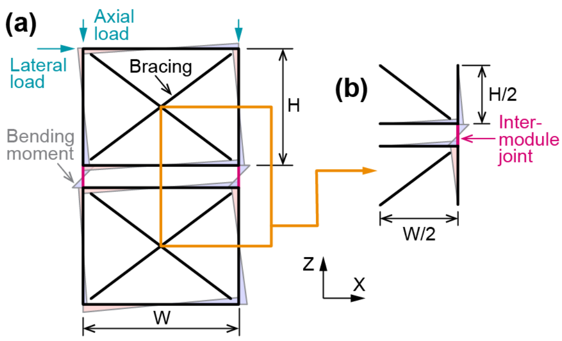

Fig. 16. (a) Braced frame showing bending moment, and (b) bending moment in beam-column subassemblage.

6.5. Stub column assembly (J/S)

The stub column assembly (Fig. 17) consists of two columns, a lower column, and an upper column, which are connected by the inter-module connection (IMC). The lower column is fixed, i.e., restrained against translation and rotation, while the top of the upper column is unrestrained to produce a cantilevered column arrangement. A lateral force is applied to the upper column causing a bending moment and a shear force to be generated in the connection. The ratio of the bending moment to the shear force can be controlled by varying the distance between the connection and the height at which the lateral (horizontal) force is applied to the upper column. In some cases, a constant axial force is applied to the upper column in addition to the lateral force.

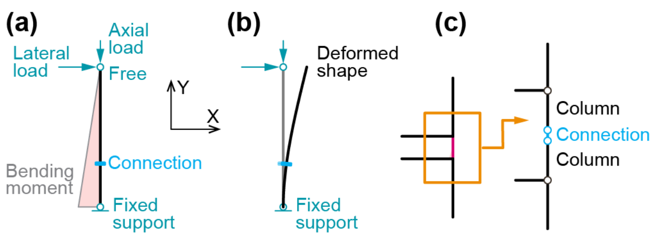

Fig. 17. Stub column assembly (J/S) showing (a) bending moment diagram, (b) deformed shape, and (c) assembly of connection and short column lengths to model joint.

For example, **Liu et al. [31]** and **Liu et al. [32]** applied this setup to establish the bending-shear performance (Fig. 18a) and the compression-bending-shear performance (Fig. 18b) of a bolted flange connection. The works established the moment-rotation (M-θ) behaviour of the connection subjected to a combined bending moment and shear force, and subjected to a combined bending moment, shear force, and axial force, respectively. Although the works were not specific to volumetric modular structures, the bolted flange connection is similar to the bolted IMCs adopted for modular buildings.

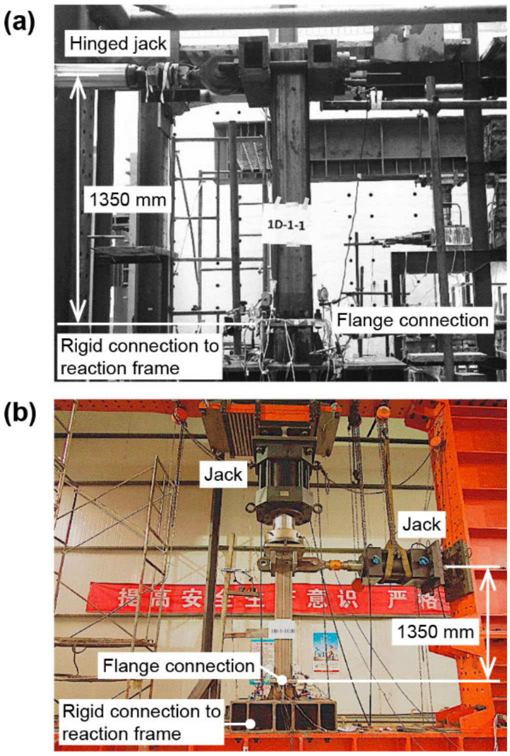

Fig. 18. Stub column assembly test for (a) bending-shear performance [31], and (b) compression-bend-shear performance of bolted flange connection [32].

Recently, i.e., 2019 to 2021, researchers have adopted this test setup for IMCs in modular buildings [33-36]. For example, **Chen et al. [33]** applied the test to establish the M-θ behaviour of the rotary connection without an axial force (Fig. 19a). The full-scale specimens were constructed from 200x18 SHS columns. The base of the column was fixed via a large 1300x600x30 mm thick steel plate with 120x6 mm thick stiffening ribs which was welded to the column and bolted to a strong floor. The middle of the new rotary connection was positioned approximately 600 mm above the floor, and the lateral load was applied a further 1200 mm above the middle of the rotary connection. Displacement sensors were installed to determine the lateral displacement at the top of the column where the lateral force was applied, and the lateral displacement, and, hence, rotation of the upper and lower halves of the rotary connection (Fig. 19b). Two inclinometers were also placed on the surface of the specimen to measure the rotation of the upper and lower corner fittings. The monotonic lateral force was applied using a hydraulic jack with load control and 5 kN increments, and loading was continued until the displacement was large, i.e., 200 mm. The rotation of the upper column relative to the lower column was calculated from the measured displacements, and the corresponding M-θ curve was reported.

In another example, **Yang [34]** adopted the stub column assembly to establish the M-θ behaviour of a semi-rigid connection for modular buildings (Fig. 20). Compared with the tests by Chen et al. [33] (Fig. 19), the length of the column cantilever was small and lateral restraint was applied at the lower beam level. As a result, when the monotonic lateral force was applied to the upper column the IMC was subjected to a small bending moment and a large shear force. The lateral displacement of the columns was measured such that the relative rotation could be calculated and, hence, the M-θ curve could be derived. It was reported that cracks initiated at the column root and that they propagated as the load was increased.

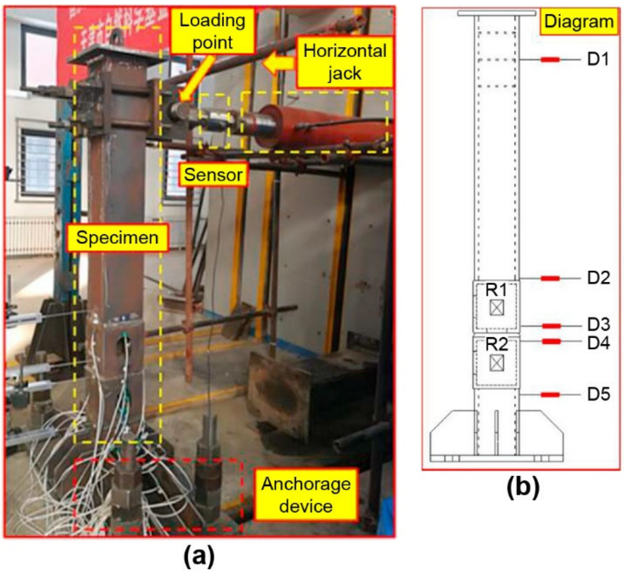

Fig. 19. Lateral loading of the rotary connection: (a) General arrangement, and (b) displacement (D) and rotation (R) measurement locations [33].

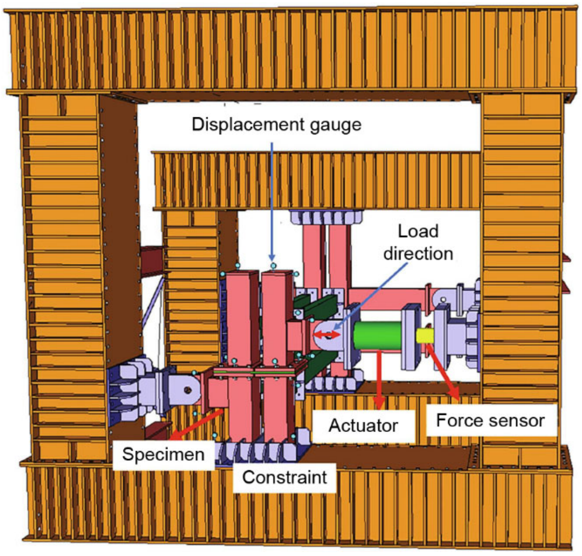

Fig. 20. Connection test for semi-rigid connection for modular buildings [34].

Similarly, **Sendanayake et al. [35]** adopted the stub column assembly to establish the monotonic and cyclic M-θ behaviours for a connection incorporating resilient layers (Fig. 21). The full-scale specimens consisted of four 150x5 SHS columns, each of which was 500 mm long. The connection between the columns was made up of a combination of 2-, 5-, and 10-mm thick steel plates, and 4.5- or 9.5-mm thick rubber layers which were clamped together by two M30 and four M20 bolts. An 810x250x36 mm thick base plate was welded to two of the columns and bolted to the test frame via eight M24 bolts. A lateral support frame provided support via rollers at the end of the other two columns, while an actuator applied the lateral force with a hinged connection between the actuator and the columns. A displacement controlled monotonic lateral force was applied to four specimens with varying steel and rubber layers forming the resilient layer, and four specimens were subjected to a cyclic lateral force using the AISC 341 [37] loading protocol. Linear variable displacement transducers, strain gauges and laser displacement sensors were adopted to measure the relative displacement between the columns and plates, strain propagation, and the global displacement, respectively. The results included normalised M-θ curves for the monotonic loading, and hysteretic M-θ curves for the cyclic loading. The reported failure modes for the monotonic and cyclic loading included yielding of the column end plates and fracture of the welds between the columns and their end plates.

As can be seen (Fig. 19 to Fig. 21), the stub column assembly test (J/S) allows variable cantilever height to account for different ratios between the bending moment and shear force in the connection. Due to this flexibility in the ratio between the bending moment and the shear force in the connection, and due to the exclusion of the beam-to-column joint (BCJ) from the specimen, the stub column assembly is particularly suited to establish the behaviour of inter-module joints (IMJs) for braced modular frames. As the BCJ does not significantly affect the lateral response of the braced frame (Section 6.4), it may be excluded from the experimental joint specimen. This, combined with the relative ease of the experiments due to the smaller specimen size, explains the increasing interest in the application of the stub column assembly for IMJs. However, the setup neglects restraint provided by the beams, and the restraints applied to the stub column do not necessarily reflect the actual modular structure. Consequently, the IMJ behaviour cannot be determined directly from the test. Instead, the J/S test can be used to determine the M-θ behaviour of the IMC. The M-θ behaviour of the IMC can then be incorporated in a global numerical model along with the additional short column lengths which make up the IMJ (Fig. 17c), as demonstrated by Lacey et al. [5]. In addition, the lateral behaviour of the IMC can be significantly affected by the applied axial force [41, 45]. Therefore, to ensure the accuracy of the structural behaviours obtained it is recommended that an axial force equal to 0.1 to 0.3 times the yield capacity of the column section, a typical range for modular buildings [3, 19], should be included in the experiments.

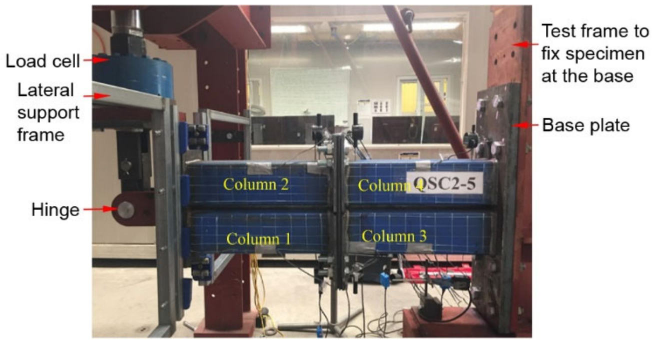

Fig. 21. Connection test which adopts the stub column assembly for a modular connection incorporating resilient layers [35].

6.6. Specimen scale

Most of the existing studies adopt full-scale specimens, and only two studies were identified which used a reduced scale (2/3) specimen for the joint tests [18, 19]. The preference for full-scale specimens can be traced to the existing standards for prequalification of connections by cyclic loading. ANSI/AISC 341 [37], for example, specifies that the depth of the beams and columns in the specimen should be at least 90% of the full-scale depth. This ensures that the specimen members are close to the full-scale size so that adverse scale effects are avoided. It is explained that deeper beams have less capacity for inelastic rotation, partly because deeper beams require larger inelastic strain for the same inelastic rotation. It is acknowledged, however, that these scale effects are not completely understood. This is certainly the case for inter-module joints (IMJs) in modular buildings for which the number of existing studies is very limited.

The existing studies undertake experiments to obtain structural behaviours which can be used to calibrate numerical models prior to parametric study. It is important, therefore, that the experimental specimen reflects the load carrying and failure mechanisms of the actual structure. To this end, a reduced-scale specimen may be adopted for experiments provided that the load carrying and failure mechanisms are similar to those of the full-scale structure. Moreover, reduced-scale tests could be encouraged, as they can enable testing of more specimens which expands the existing literature and is useful in the development of new IMJs. Nevertheless, it should be acknowledged that it may be difficult to ensure similarity of the failure mechanisms between the reduced- and full-scale specimens. The full-scale failure mechanisms may only be revealed by full-scale experiments, which could be undertaken following refinement of the new IMJ design based on a number of reduced-scale experiments.

7. Loading protocol

The experiments discussed in Sections 4, 5, and 6 focused mainly on the performance of modular joints subjected to monotonic and cyclic lateral actions. Different studies adopted different standards for the associated loading protocols. Table 3 lists the standards adopted in the existing studies, and Fig. 22 illustrates the corresponding cyclic loading protocols. The Korean Building Code (KBC) [52] and AISC 341 [37] cyclic loading protocols are effectively the same, and this loading protocol was adopted by the largest number of the existing studies, i.e., five studies. In comparison, the ATC-24 [46] and JGJ 101-96 [43] standards were each adopted by four studies.

Table 3. Standards adopted in the existing studies for the cyclic loading protocol.

Standard	Illustration	Ref.	Test Type
Korean Building Code (KBC) [52]	Fig. 22(a)	[22-24]	J/C, J/B
Seismic provisions for structural steel buildings (ANSI/AISC 341, US standard) [37]	Fig. 22(a)	[20, 35]	J/C, J/S
Regulations of seismic test method (JGJ 101-96, Chinese standard) [43]	Fig. 22(b)	[14, 18, 19, 30]	M, J/C, J/B
Guidelines for cyclic seismic testing of components of steel structures (ATC-24, US standard) [46]	Fig. 22(c)	[17, 25-27]	F, J/B

ATC-24 [46], one of the first protocols developed for steel components [53], adopts a protocol based on the yield deformation, Δy, which was developed based on statistical analysis of the global drift of single degree of freedom (SDOF) systems. First, the yield displacement is determined either by applying established design equations, or by analysing the results of a monotonic test. In the existing studies [25-27], load-controlled monotonic tests are carried out and the yield load, Qy, is set as 70% of the ultimate load. After the yield displacement is established, a new specimen is subjected to cyclic loading. Six elastic cycles are applied with an amplitude less than Δy. These elastic cycles are carried out using load control, and three cycles are required to have an amplitude of 0.75Qy, where Qy is the yield load from the monotonic test. To complete the six elastic cycles, ATC-24 shows three initial cycles with an amplitude of 0.5Qy. The displacement controlled inelastic cycles follow with three cycles per increment at amplitudes of Δy, $2\Delta y$, and $3\Delta y$. Thereafter the amplitude is increased in increments of Δy with two cycles per increment, until severe strength deterioration is encountered. The existing studies [25-27] terminated the test when the lateral load dropped below 85% of the maximum value.

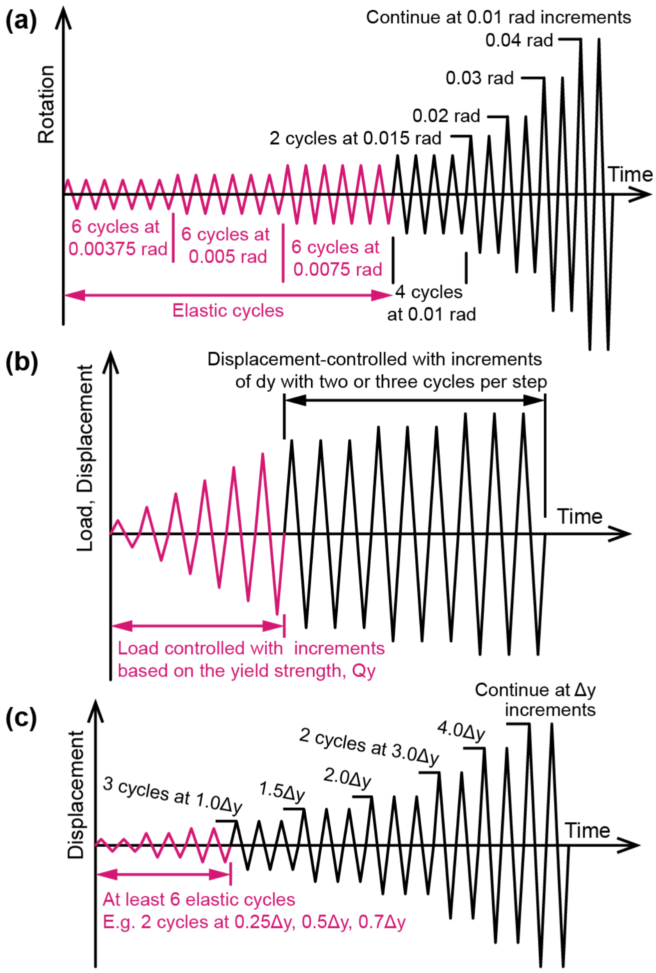

Fig. 22. Cyclic loading protocol from (a) Korean Building Code [52] and ANSI/AISC 341 (US standard) [37], (b) JGJ 101-96 (Chinese standard) [43], and (c) ATC-24 (US standard) [46]. Qy is the yield strength and Δy is the corresponding yield displacement from the monotonic test.

The existing studies which cite the ATC-24 standard [25-27] deviate slightly from the standard loading protocol. Firstly, the elastic cycles were conducted using displacement control rather than load control. This is not recommended by ATC-24 as the high initial stiffness of the specimen for the early elastic cycles can result in small displacements which are difficult to measure and control with sufficient accuracy. Secondly, the elastic cycles consist of two cycles at 0.25Δy, 0.5Δy, and 0.7Δy (Fig. 22c). Although the required total of six elastic cycles is satisfied, the requirement for three cycles with an amplitude of 0.75Qy is not met. ATC-24 suggests that the yield displacement can be estimated from the monotonic test based on a control deformation δ* which is defined as the deformation for a load of 0.75Qy. Therefore, the three cycles at 0.75Qy serve to verify the control deformation for the specimen subjected to cyclic loading. Since the existing studies [25-27] did not estimate the yield displacement using the ATC-24 suggested method, it is reasonable that the largest elastic cycles were carried out for an amplitude of 0.7Δy. Finally, the existing studies [25-27] introduce an intermediate amplitude of 1.5Δy. This is generally consistent with other loading protocols such as AISC 341 [37] which, apart from introducing a larger number of elastic cycles to account for the possibility of weld fracture during the elastic cycles, introduce cycles at an intermediate amplitude of 0.015 rad [53].

There are two main issues with the ATC-24 loading protocol and other protocols which similarly define the cyclic load based on the yield displacement, e.g., JGJ 101-96 [43]. Firstly, the ambiguity of the yield displacement can lead to inconsistency between different researchers which in turn can lead to results which are difficult to compare [53]. Secondly, the ATC-24 (Fig. 22c) and JGJ 101-96 (Fig. 22b) loading protocols have only a small number of elastic cycles, i.e., six cycles. This might not be sufficient to identify the potential for weld fracture in the beam-to-column joints (BCJs) during the elastic cycles. For these reasons it is recommended that more recent protocols, such as the AISC 341 [37] loading protocol, are adopted in preference to either ATC-24 or JGJ 101-96.

AISC 341 [37] incorporates the standard SAC loading protocol [54] for steel moment connections in beam-column subassemblages which was developed based on the inter-storey drift angle, θ [53]. The test consists of six cycles of each of the amplitudes of 0.00375, 0.005, and 0.0075 rad, then four cycles with an amplitude of 0.01 rad, followed by two cycles for each of the amplitudes of 0.015, 0.02, 0.03, and 0.04 rad (Fig. 22a). The cycles then continue at 0.01 rad increments with two cycles per step, until the axial force or the lateral force drops below 80% of the maximum value [53]. In traditional steel frame structures the drift at which the storey yields is typically close to 0.01 rad [53]. Thus, the cycles with an amplitude of 0.00375, 0.005, and 0.0075 rad are typically elastic cycles, while the following cycles at 0.01 rad and above represent the inelastic stage. The main advantage of the standard SAC loading protocol incorporated in AISC 341, other than the larger number of elastic cycles and intermediate 0.015 rad amplitude cycles, is the use of the inter-storey drift as the control parameter. This means, firstly, that the same increment amplitudes will be applied consistently by different researchers, and, secondly, that the loading protocol is defined without the need for prior monotonic tests. Nevertheless, as done in the existing study [35], it is recommended that monotonic tests are carried out in addition to the cyclic tests. In this way the cyclic strength deterioration and yield strength of the new modular joints can be well established.

The cyclic loading is typically applied slowly to avoid dynamic effects [20, 55], that is, to give the quasi-static behaviour without significant strain rate effects nor inertia resistance. A faster rate of loading may, however, be required to complete the required cycles in a reasonable time. For a beam-column subassemblage with column loading (J/C), Sanches et al. [20] adopted rates of 0.35 to 1.5 mm/s, while Lee et al. [22] applied 0.05 mm/s to a maximum of 110 mm (0.05 rad). For the tests with beam loading (J/B), Lee et al. [24] applied up to 140 mm (0.075 rad) at a rate of 0.25 to 1.0 mm/s. In another study, Annan et al. [55] investigated the seismic performance of modular steel-braced frames and applied loads at a rate of 3.5 to 4.0 kN/s for the elastic cycles and 1.8 to 2.2 mm/s for the inelastic cycles. Thus, there is significant variation in the loading rates, i.e., 0.05 to 2.2 mm/s. At the upper end (2.2 mm/s), the loading rate is relatively high compared with the recent literature for other structures. For example, Elflah et al. [56] adopted a loading rate of 1.0 to 1.5 mm/min (0.017 to 0.025 mm/s) to establish the moment-rotation (M-θ) behaviour of stainless steel beam-to-tubular column joints, while Ngo et al. [57] used rates of 6 to 9 mm/min (0.1 to 0.15 mm/s) to establish the cyclic performance of monolithic and non-corrosive dry geopolymer concrete BCJs. Hence, while rates of 3 to 132 mm/min are supported by the existing literature, 1 to 9 mm/min (0.017 to 0.15 mm/s) is suggested as a starting point to obtain the quasi-static behaviour of IMJs.

For the monotonic loading, a linearly increasing lateral load is applied to the specimen. The lateral load can be either load-controlled or displacement-controlled, and it is typically increased until the lateral load drops below 85% of the maximum value [27]. According to the standard ATC-24 [46] the lateral load should be load-controlled as the high stiffness of the specimen prior to yield leads to small displacements which are difficult to measure accurately. However, no guidance is provided on the rate of loading. As mentioned, Annan et al. [55] adopted a rate of 3.5 to 4.0 kN/s for the elastic behaviour of modular steel-braced frames, however, this could be too fast to guarantee a quasi-static response from the inter-module joint. Alternatively, if the laboratory can accommodate it, displacement-controlled loading could be adopted for which a rate of 1 to 9 mm/min (0.017 to 0.15 mm/s) is suggested.

8. Recommendations for future work

Table 4 summarises the advantages and disadvantages of the experimental methods reviewed in Sections 4, 5, and 6. To standardise future works, joint tests adopting the beam-column (BC) subassemblage with column loading (J/C) are recommended to establish the IMJ behaviour for unbraced modular frames. The geometry of the unbraced modular frame, based on which the BC subassemblage was defined, should be reported. The beam-to-column joints (BCJs) should be strengthened as required to ensure adequate performance of the prototype and to reveal the IMJ behaviour in the joint tests. Roller supports are recommended for the beam ends, rather than hinged struts which constrain the lateral movement and can influence the IMJ behaviour. Beam loading (J/B) is not recommended; however, such tests could be adopted if it can be demonstrated that the IMJ behaviour is not significantly affected by the different deformed shape of the specimen which results from the different boundary conditions. For the development of new IMJs, reduced scale experimental specimens are suggested for tests undertaken to calibrate the associated numerical models, provided that the load carrying, and failure mechanisms reflect those in the full-scale structure. If, however, the tests are undertaken for prequalification of the BCJ, then full-scale specimens should comply with the relevant standard, such as ANSI/AISC 341 [37].

Use of the stub column assembly (J/S) is recommended for the assessment of IMJs in braced modular frames. It should be acknowledged that the J/S test cannot determine the IMJ behaviour directly. Rather, the J/S test determines the IMC behaviour which can be incorporated in global numerical models along with additional short column lengths as required to complete the IMJ. Consequently, the J/S test could be seen as a test of the IMCs which can be undertaken to determine either the M-θ or the shear force-displacement behaviour under different combined loading conditions. Otherwise, pure shear tests [40, 48] may be undertaken to establish the pure shear behaviour of the IMC.

To give the most realistic joint behaviour it is suggested that the joint tests should generally be completed with an axial force of 0.1 to 0.3 times the column yield capacity [3, 19]. This follows the modular structures with the largest shear forces occurring in the IMJs at the building base where the axial forces due to self-weight are the largest. Monotonic tests are recommended for the J/C and J/S tests to establish the yield capacity of the new modular joints. The loading should be continued until the lateral load drops below 85% of the maximum value. The tests could be load-controlled, and the existing literature suggests a rate of 3.5 to 4.0 kN/s, however, this could be too fast to ensure quasi-static responses in all cases. Alternatively, if possible, a displacement controlled protocol could be adopted with a rate of 1 to 9 mm/min. Cyclic tests are also recommended for the J/B and J/S tests following the AISC 341 [37] standard. This standard includes a larger number of elastic cycles to identify the potential for weld fracture in the BCJs and adopts inter-storey drift as the control parameter. Displacement-controlled loading at a rate of 1 to 9 mm/min is suggested for the cyclic tests, continued until the lateral load drops below 85% of the maximum value.

Table 4. Summary of the different tests undertaken in the existing literature to determine the structural behaviours of inter-module joints (IMJs)

Test Type	Sub-type	Advantages	Disadvantages
Module (M)	-	**Most accurate** assessment of IMJ behaviour including interaction with other elements such as the BCJ.	**Most expensive** method due to size of prototype specimen and test facilities required. IMJ behaviour within module can be affected by other elements such as the BCJs. The existing literature is limited to three studies on unbraced modular frames.
Frame (F)	-	**Accurate** assessment of **in-plane** IMJ behaviour. **Less expensive than module test** due to smaller size of frame compared with module.	**Still expensive** due to the size of the prototype specimens and the facilities required. **Reduction to frame substructure** may not capture three-dimensional module behaviour, and requires out of plane restraint.
Joint (J)	Beam-column subassemblage with column loading (J/C)	Assessment of IMJ behaviour including the BCJs. **Less expensive than frame test** as joint specimens are smaller than frame specimens. **Recommended for unbraced modular frames.**	Resulting behaviour of the IMJ is specific to the defined unbraced transverse frame geometry, and may not be extrapolated to other frame geometries. Displacement and ultimate failure may be **controlled by the BCJ rather than the IMJ.**
	Beam-column subassemblage with beam loading (J/B)	**Less expensive than joint (J/C) test** as restraint at top of column allows simpler setup for application of axial load. **Can reproduce design actions** in members, i.e., design actions equivalent to joint (J/C) test	**Cannot reproduce deformed shape** due to different boundary conditions which can affect the IMJ behaviour. Cannot reproduce nonlinear effects such as the P-Delta effect.
	Stub column assembly (J/S)	**Least expensive** due to the small specimen size. **Flexible geometry** depending on height between modules or otherwise to model different ratios between shear force and bending moment induced in the IMC. Hence, combined loading (shear/bending) can be considered. **Recommended for braced modular frames.**	**Neglects restraint** provided by beams, and restraints to stub column may not reflect the actual modular structure. **IMJ behaviour cannot be determined directly**. Instead, the J/S test determines the IMC behaviour which can be incorporated in global numerical models. Additional steel members may be required to complete the IMJ model.

9. Concluding remarks

The experimental methods for inter-module joints (IMJs) in modular buildings have been comprehensively summarised and discussed in this paper. The main findings and future research directions are summarised as follows.

1. The module (M) tests are expensive due to the size of the specimen and the facilities required. Moreover, it can be difficult to separate the IMJ and beam-to-column joint (BCJ) behaviours which are incorporated within the measured lateral displacements. However, the module (M) tests include all the key structural elements and offer the most accurate assessment of the IMJ behaviour and its effect on the overall building

response. The existing literature is very limited, i.e., only three studies, and focussed on the response of unbraced modular steel frames to quasi-static actions. Due to the accuracy, the module test is recommended for new types of modular structures, and structures subjected to combined, biaxial and dynamic actions. Apart from developing knowledge on the specific structural behaviours, such studies could further establish the requirements for the following substructure tests.

2. The frame (F) tests offer a reasonable estimate of the in-plane joint behaviour but neglect global failure modes which might occur in the complete structure. Moreover, although the frame specimens are smaller than the module specimens, they are still relatively large and expensive in terms of the materials and facilities required. The existing literature is extremely limited, i.e., only one study which investigated the IMJ behaviour for a particular IMC, and demonstrated that the joint behaviour can differ between the braced and unbraced structures. In other cases, however, it may be sufficient to adopt a joint (J) test with appropriate loading and boundary conditions.

3. For the joint (J) tests, the beam-column subassemblages and stub column assemblies are smaller and more cost effective than the module and frame specimens. Joint tests adopting the beam-column (BC) subassemblage with column loading (J/C) are recommended to establish the IMJ behaviour for unbraced modular frames, whereas the stub column assembly (J/S) is recommended for braced modular frames. Section 8 gives a summary of the recommendations to standardise the application of such joint tests.

4. The existing literature focuses on modular structures with a very small or zero gap between the floor and ceiling beams. Further study is needed for structures with a larger gap between the beams. This would allow services to run between the beams, thereby allowing greater flexibility in the layout of services and, hence, greater flexibility in the modular floor plans.

5. The existing experimental works focus on the response to quasi-static uniaxial monotonic and cyclic lateral loads. Experimental methods for biaxial lateral and dynamic actions remain to be developed.

10. CRediT authorship contribution statement

Andrew Lacey: Conceptualization, Investigation, Formal analysis, Visualization, Writing - original draft. **Wensu Chen:** Funding acquisition, Supervision, Validation, Writing - review & editing. **Hong Hao:** Supervision, Validation, Writing - review & editing.

11. Declaration of Competing Interest

The authors declare that they have no known competing financial interests or personal relationships that could have appeared to influence the work reported in this paper.

12. Acknowledgements

The second author acknowledges the financial support from the Australian Government through the Australian Research Council (ARC) Future Fellowship (FT210100050).

13. References

[1] CEN. EN 1993-1-8:2005 Eurocode 3: Design of steel structures - Part 1-8: Design of joints. Brussels, Belgium: European Committee for Standardization (CEN); 2005.

[2] Lacey AW, Chen W, Hao H, Bi K. Structural response of modular buildings - an overview. J Build Eng. 2018;16:45-56. https://doi.org/10.1016/j.jobe.2017.12.008

[3] Lacey AW, Chen W, Hao H, Bi K. Review of bolted inter-module connections in modular steel buildings. J Build Eng. 2019;23:207-19. https://doi.org/10.1016/j.jobe.2019.01.035

[4] Lacey AW, Chen W, Hao H, Bi K. Effect of inter-module connection stiffness on structural response of a modular steel building subjected to wind and earthquake load. Eng Struct. 2020;213:110628. https://doi.org/10.1016/j.engstruct.2020.110628

[5] Lacey AW, Chen W, Hao H, Bi K. Lateral behaviour of modular steel building with simplified models of new inter-module connections. Eng Struct. 2021;236:112103. https://doi.org/10.1016/j.engstruct.2021.112103

[6] Lawson RM, Ogden RG, Goodier C. Design in Modular Construction. Boca Raton, FL, USA: CRC Press; 2014.

[7] Ferdous W, Bai Y, Ngo TD, Manalo A, Mendis P. New advancements, challenges and opportunities of multi-storey modular buildings – A state-of-the-art review. Eng Struct. 2019;183:883-93. https://doi.org/10.1016/j.engstruct.2019.01.061

[8] Srisangeerthanan S, Hashemi MJ, Rajeev P, Gad E, Fernando S. Review of performance requirements for inter-module connections in multi-story modular buildings. J Build Eng. 2020;28:101087. https://doi.org/10.1016/j.jobe.2019.101087

[9] Deng E-F, Zong L, Ding Y, Zhang Z, Zhang J-F, Shi F-W et al. Seismic performance of mid-to-high rise modular steel construction - A critical review. Thin Wall Struct. 2020;155:106924. https://doi.org/10.1016/j.tws.2020.106924

[10] Thai H-T, Ngo T, Uy B. A review on modular construction for high-rise buildings. Structures. 2020;28:1265-90. https://doi.org/10.1016/j.istruc.2020.09.070

[11] Nadeem G, Safiee NA, Bakar NA, Karim IA, Nasir NAM. Connection design in modular steel construction: A review. Structures. 2021;33:3239-56. https://doi.org/10.1016/j.istruc.2021.06.060

[12] Chen Z, Khan K, Khan A, Javed K, Liu J. Exploration of the multidirectional stability and response of prefabricated volumetric modular steel structures. J Constr Steel Res. 2021;184:106826. https://doi.org/10.1016/j.jcsr.2021.106826

[13] Hong S-G, Cho B-H, Chung K-S, Moon J-h. Behavior of framed modular building system with double skin steel panels. J Constr Steel Res. 2011;67:936-46. https://doi.org/10.1016/j.jcsr.2011.02.002

[14] Chen Z, Li H, Chen A, Yu Y, Wang H. Research on pretensioned modular frame test and simulations. Eng Struct. 2017;151:774-87. https://doi.org/10.1016/j.engstruct.2017.08.019

[15] Lyu Y-F, Li G-Q, Cao K, Zhai S-Y, Li H, Chen C et al. Behavior of splice connection during transfer of vertical load in full-scale corner-supported modular building. Eng Struct. 2021;230:111698. https://doi.org/10.1016/j.engstruct.2020.111698

[16] Liu Y, Chen Z, Liu J, Bai Y, Zhong X, Wang X. Lateral stiffness evaluation on corner-supported thin walled modular steel structures. Thin Wall Struct. 2020;157:106967. https://doi.org/10.1016/j.tws.2020.106967

[17] Liu J, Chen Z, Liu Y, Bai Y, Zhong X. Full-scale corner-supported modular steel structures with vertical inter-module connections under cyclic loading. J Build Eng. 2021;44:103269. https://doi.org/10.1016/j.jobe.2021.103269

[18] Chen Z, Liu J, Yu Y, Zhou C, Yan R. Experimental study of an innovative modular steel building connection. J Constr Steel Res. 2017;139:69-82. https://doi.org/10.1016/j.jcsr.2017.09.008

[19] Chen Z, Liu J, Yu Y. Experimental study on interior connections in modular steel buildings. Eng Struct. 2017;147:625-38. https://doi.org/10.1016/j.engstruct.2017.06.002

[20] Sanches R, Mercan O, Roberts B. Experimental investigations of vertical post-tensioned connection for modular steel structures. Eng Struct. 2018;175:776-89. https://doi.org/10.1016/j.engstruct.2018.08.049

[21] Cho B-H, Lee J-S, Kim H, Kim D-J. Structural Performance of a New Blind-Bolted Frame Modular Beam-Column Connection under Lateral Loading. Applied Sciences. 2019;9. https://doi.org/10.3390/app9091929

[22] Lee S-S, Park K-S, Jung J-S, Lee K-S. Evaluation of the Structural Performance of a Novel Methodology for Connecting Modular Units Using Straight and Cross-Shaped Connector Plates in Modular Buildings. Applied Sciences. 2020;10. https://doi.org/10.3390/app10228186

[23] Lee S, Park J, Kwak E, Shon S, Kang C, Choi H. Verification of the seismic performance of a rigidly connected modular system depending on the shape and size of the ceiling bracket. Materials. 2017;10:263. https://doi.org/10.3390/ma10030263

[24] Lee S, Park J, Shon S, Kang C. Seismic performance evaluation of the ceiling-bracket-type modular joint with various bracket parameters. J Constr Steel Res. 2018;150:298-325. https://doi.org/10.1016/j.jcsr.2018.08.008

[25] Deng E-F, Zong L, Ding Y, Dai XM, Lou N, Chen Y. Monotonic and cyclic response of bolted connections with welded cover plate for modular steel construction. Eng Struct. 2018;167:407-19. https://doi.org/10.1016/j.engstruct.2018.04.028

[26] Deng E-F, Zong L, Ding Y, Luo Y-B. Seismic behavior and design of cruciform bolted module-to-module connection with various reinforcing details. Thin Wall Struct. 2018;133:106-19. https://doi.org/10.1016/j.tws.2018.09.033

[27] Dai X-M, Zong L, Ding Y, Li Z-X. Experimental study on seismic behavior of a novel plug-in self-lock joint for modular steel construction. Eng Struct. 2019;181:143-64. https://doi.org/10.1016/j.engstruct.2018.11.075

[28] Wang Y, Xia J, Ma R, Xu B, Wang T. Experimental Study on the Flexural Behavior of an Innovative Modular Steel Building Connection with Installed Bolts in the Columns. Applied Sciences. 2019;9. https://doi.org/10.3390/app9173468

[29] Ma R, Xia J, Chang H, Xu B, Zhang L. Experimental and numerical investigation of mechanical properties on novel modular connections with superimposed beams. Eng Struct. 2021;232:111858. https://doi.org/10.1016/j.engstruct.2021.111858

[30] Chen Z, Wang J, Liu J, Khan K. Seismic behavior and moment transfer capacity of an innovative self-locking inter-module connection for modular steel building. Eng Struct. 2021;245:112978. https://doi.org/10.1016/j.engstruct.2021.112978

[31] Liu XC, He XN, Wang HX, Yang ZW, Pu SH, Ailin Z. Bending-shear performance of column-to-column bolted-flange connections in prefabricated multi-high-rise steel structures. J Constr Steel Res. 2018;145:28-48. https://doi.org/10.1016/j.jcsr.2018.02.017

[32] Liu XC, He XN, Wang HX, Zhang AL. Compression-bend-shearing performance of column-to-column bolted-flange connections in prefabricated multi-high-rise steel structures. Eng Struct. 2018;160:439-60. https://doi.org/10.1016/j.engstruct.2018.01.026

[33] Chen Z, Liu Y, Zhong X, Liu J. Rotational stiffness of inter-module connection in mid-rise modular steel buildings. Eng Struct. 2019;196:109273. https://doi.org/10.1016/j.engstruct.2019.06.009

[34] Yang H. Performance analysis of semi-rigid connections in prefabricated high-rise steel structures. Structures. 2020;28:837-46. https://doi.org/10.1016/j.istruc.2020.09.036

[35] Sendanayake SV, Thambiratnam DP, Perera NJ, Chan THT, Aghdamy S. Enhancing the lateral performance of modular buildings through innovative inter-modular connections. Structures. 2021;29:167-84. https://doi.org/10.1016/j.istruc.2020.10.047

[36] Lyu Y-F, Li G-Q, Cao K, Zhai S-Y, Wang Y-B, Mao L et al. Bending behavior of splice connection for corner-supported steel modular buildings. Eng Struct. 2022;250:113460. https://doi.org/10.1016/j.engstruct.2021.113460

[37] AISC. ANSI/AISC 341-16 Seismic Provisions for Structural Steel Buildings. Chicago, Illinois, USA: American Institute of Steel Construction (AISC); 2016.

[38] Alembagheri M, Sharafi P, Hajirezaei R, Tao Z. Anti-collapse resistance mechanisms in corner-supported modular steel buildings. J Constr Steel Res. 2020;170:106083. https://doi.org/10.1016/j.jcsr.2020.106083

[39] Luo FJ, Bai Y, Hou J, Huang Y. Progressive collapse analysis and structural robustness of steel-framed modular buildings. Eng Fail Anal. 2019;104:643-56. https://doi.org/10.1016/j.engfailanal.2019.06.044

[40] Lacey AW, Chen W, Hao H, Bi K, Tallowin FJ. Shear behaviour of post-tensioned inter-module connection for modular steel buildings. J Constr Steel Res. 2019;162:105707. https://doi.org/10.1016/j.jcsr.2019.105707

[41] Lacey AW, Chen W, Hao H, Bi K. Simplified structural behaviours of post-tensioned inter-module connection for modular buildings. J Constr Steel Res. 2020;175:106347. https://doi.org/10.1016/j.jcsr.2020.106347

[42] Peng J, Hou C, Shen L. Numerical simulation of weld fracture using cohesive interface for novel inter-module connections. J Constr Steel Res. 2020;174:106302. https://doi.org/10.1016/j.jcsr.2020.106302

[43] Ministry of Construction. JGJ 101-96 Specification of testing methods for earthquake resistant building. Beijing, China: China Architecture & Building Press; 1996.

[44] AISC. ANSI/AISC 341-05 Seismic Provisions for Structural Steel Buildings. Chicago, Illinois, USA: American Institute of Steel Construction (AISC); 2005.

[45] Lacey AW, Chen W, Hao H, Bi K. New interlocking inter-module connection for modular steel buildings: Simplified structural behaviours. Eng Struct. 2021;227:111409. https://doi.org/10.1016/j.engstruct.2020.111409

[46] ATC. Guidelines for Cyclic Seismic Testing of Components of Steel Structures, ATC 24. Redwood City, CA, USA: Applied Technology Council (ATC); 1992.

[47] Lacey AW, Chen W, Hao H, Bi K. Experimental and numerical study of the slip factor for G350-steel bolted connections. J Constr Steel Res. 2019;158:576-90. https://doi.org/10.1016/j.jcsr.2019.04.012

[48] Lacey AW, Chen W, Hao H, Bi K. New interlocking inter-module connection for modular steel buildings: Experimental and numerical studies. Eng Struct. 2019;198:109465. https://doi.org/10.1016/j.engstruct.2019.109465

[49] Genesio G. Seismic Assessment of RC Exterior Beam-Column Joints and Retrofit with Haunches Using Post-Installed Anchors [PhD Thesis]. Germany: University of Stuttgart; 2012.

[50] Zhang G, Xu L-H, Li Z-X. Development and seismic retrofit of an innovative modular steel structure connection using symmetrical self-centering haunch braces. Eng Struct. 2021;229:111671. https://doi.org/10.1016/j.engstruct.2020.111671

[51] Sanches R, Tao J, Fathieh A, Mercan O. Investigation of the seismic performance of braced low-, mid- and high-rise modular steel building prototypes. Eng Struct. 2021;234:111986. https://doi.org/10.1016/j.engstruct.2021.111986

[52] AIK. Korean Building Code and Commentary - Structural. Seoul, Korea: Architectural Institute of Korea (AIK); 2016.

[53] Krawinkler H. Loading histories for cyclic tests in support of performance assessment of structural components. The 3rd international conference on advances in experimental structural engineering (3AESE); October 15-16; San Francisco, CA, United States2009.

[54] Clark P, Frank K, Krawinkler H, Shaw R. SAC/BD-97/02 Protocol for Fabrication, Inspection, Testing, and Documentation of Beam-Column Connection Tests and Other Experimental Specimens. Sacramento, CA, United States: SAC Joint Venture; 1997.

[55] Annan CD, Youssef MA, El Naggar MH. Experimental evaluation of the seismic performance of modular steel-braced frames. Eng Struct. 2009;31:1435-46. https://doi.org/10.1016/j.engstruct.2009.02.024

[56] Elflah M, Theofanous M, Dirar S, Yuan H. Structural behaviour of stainless steel beam-to-tubular column joints. Eng Struct. 2019;184:158-75. https://doi.org/10.1016/j.engstruct.2019.01.073

[57] Ngo TT, Tran TT, Pham TM, Hao H. Performance of geopolymer concrete in monolithic and non-corrosive dry joints using CFRP bolts under cyclic loading. Compos Struct. 2021;258:113394. https://doi.org/10.1016/j.compstruct.2020.113394